AD-A163 975 THE EFFECT OF ENERGY DISSIPATION DUE TO FRICTION AT THE 1/1
JOINT OF A SIMPLE.. (U) AIR FORCE INST OF TECH
WRIGHT-PATTERSON AFB OH SCHOOL OF ENGI.. R P DONNELLY
UNCLASSIFIED DEC 85 AFIT/GAE/AA/85D-5 F/G 22/2 NL

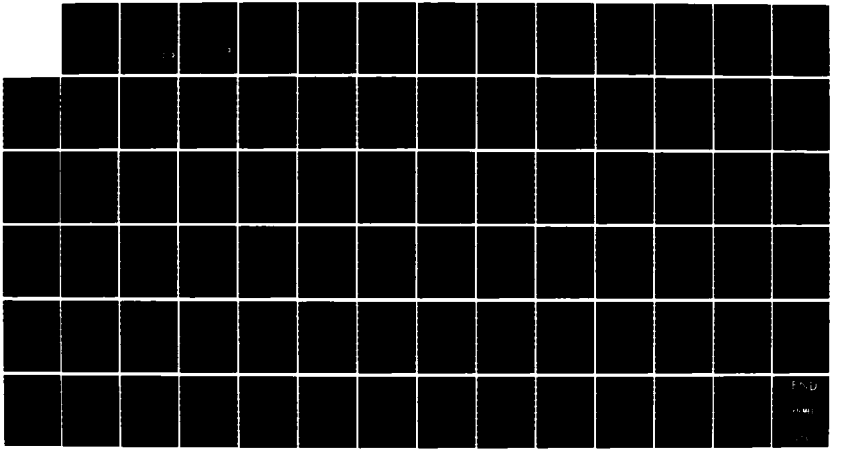

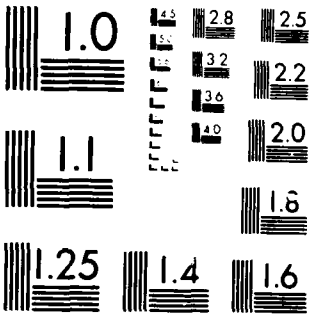

MICROCOPY RESOLUTION TEST CHART
NATIONAL BUREAU OF STANDARDS 1963-A

AD-A163 975

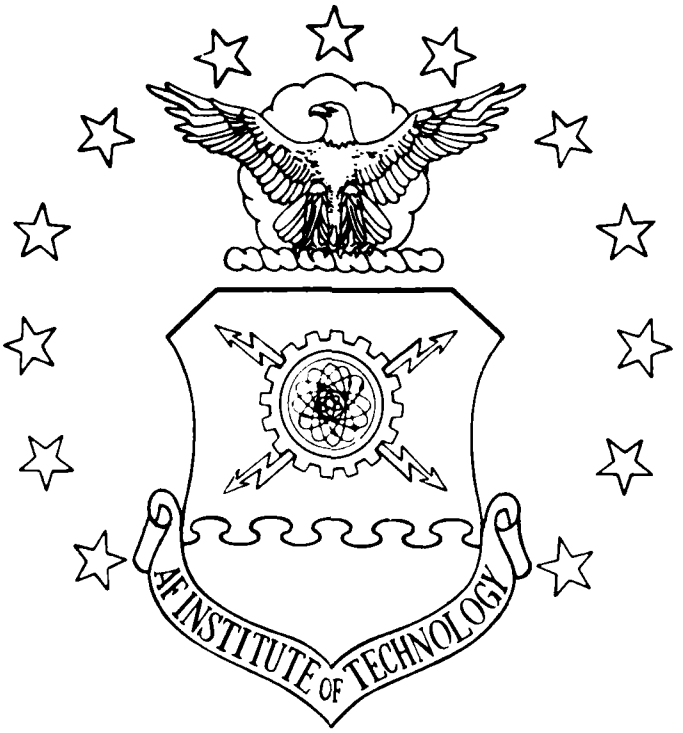

THE EFFECT OF ENERGY DISSIPATION DUE TO FRICTIO AT THE JOINT OF A SIMPLE BEAM STRUCTURE

THESIS

Robert I. Donnelly, Jr.
Captain, USAF

AFIT/GAE/AA/85D-5

DTIC FILE COPY

DISTRIBUTION STATEMENT A
Approved for public release
Distribution Unlimited

DTIC
ELECTE
FEB 1 2 1986
S D
B

DEPARTMENT OF THE AIR FORCE
AIR UNIVERSITY
AIR FORCE INSTITUTE OF TECHNOLOGY

Wright-Patterson Air Force Base, Ohio

86 2 12 055

AFIT/GAE/AA/85D-5

THE EFFECT OF ENERGY DISSIPATION DUE TO FRICTION AT THE JOINT OF A SIMPLE BEAM STRUCTURE

THESIS

Robert F. Donnelly, Jr.
Captain, USAF

AFIT/GAE/AA/85D-5

DTIC
ELECTE
FEB 1 2 1986
S D
B

Approved for public release; distribution unlimited

LIST OF FIGURES

ACKNOWLEDGEMENTS

I would like to express my sincere gratitude to Capt. Ron Hinrichsen for never giving up on this project, even in its darkest moments. His patience, technical guidance, encouragement, and time spent gave me the will to go on when I considered throwing in the towel. A special thanks to Capt. Lanny Hudson who spent some of his own time with this study despite not being assigned to the committee.

Finally, my sincerest gratitude and affection for my wife and family, who bore the brunt of the early failings of this thesis, but were always there with a kind word when I needed it most.

Robert P. Donnelly, Jr.

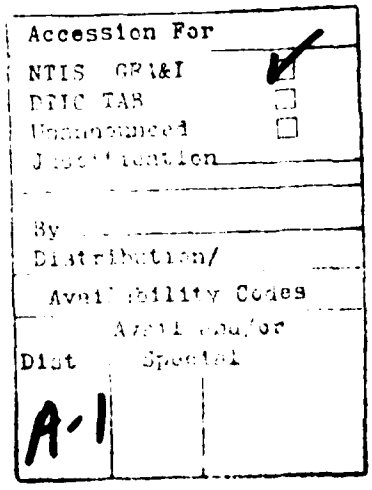

AFIT/GAE/AA/85D-5

THE EFFECTS OF ENERGY DISSIPATION DUE TO FRICTION AT THE JOINT OF A SIMPLE BEAM STRUCTURE

THESIS

Presented to the Faculty of the School of Engineering

of the Air Force Institute of Technology

Air University

In Partial Fulfillment of the

Requirements for the Degree of

Master of Science in Aeronautical Engineering

Robert P. Donnelly, Jr.

Captain, USAF

December 1985

Approved for public release; distribution unlimited

TABLE OF CONTENTS

LIST OF TABLES

ABSTRACT

The Strategic Defense Initiative has generated new interest in the development of more stable space structures. This interest has increased the need for more detailed knowledge of the behavior of engineering structures under dynamic loading. Interests lie in decreasing the amount of vibration by both passively and actively damping the structure. A means exists to passively damp structures by friction damping resulting from relative slip between joint interfaces. It may be feasible to increase the damping in a structure by allowing more friction damping than is normal and thereby controlling the vibration response.

This study incorporates friction damping in a one-dimensional model. Finite element techniques are used to accomplish the numerical analysis. A clamped-clamped beam is used as the physical model. The mid-point of the two element beam is allowed to slip in rotation, but not in translation. Because the one-dimensional program cannot handle rotations at continous nodes, the beam is modeled by symmetry about the joint and a cantilever beam with an applied end moment is studied.

Results for the response of a beam in vibration are presented showing displacement of the joint, relative rotation at the joint, and relative angular velocity at the joint; all versus time. Various clamping pressures and

initial loads are explored. Diagrams of the beam shape vs. time show the shape the beam takes on when slip occurs at the joint. Frequency calculations show that the period of the response is affected by clamping pressure, but not by the initial loading. Energy loss calculations are presented for various clamping pressures.

CHAPTER 1

INTRODUCTION

1.1 BACKGROUND

There has been an increase in interest in the stability of large space structures due to the Strategic Defense Initiative (SDI). A desire exists to mount sensitive equipment (tracking and reflecting devices) externally on these structures. The rotation of these structures could cause vibrations to occur which, if unchecked, could significantly affect the accuracy of the mounted equipment.

Space structures operate in an environment offering no aerodynamic damping. In addition, the use of low mass and all-welded construction methods, lacking sufficient inherent damping, decrease the ability of the structures to reduce unwanted vibrations (19). Thus, expensive and complex damping systems are needed to achieve the desired levels of damping. However, friction damping is a method available to passively damp vibrations in structures, thereby reducing the need for these active damping systems.

Friction damping, the interfacial slip in the joints of a structure, is the major contributor to the inherent damping of a structure. Usually over 90 percent of the damping in structures takes place in the joints (2). Three primary reasons are given for not relying on this mechanism in the past. First, the small movements between the

surfaces of the joint can cause fretting corrosion, leading to fatigue and possible failure of the joint or structure. Second, by decreasing the stiffness in the joint in order to permit slip, a relative loss of static stiffness of the structure is realized. Finally, and probably the most influential reason, friction forces in the joint are non-linear. It is, therefore, difficult to determine the force transmitted across the joint and to predict the effect on the vibration response of a structure. As a result of these disadvantages of friction damping, joints are normally clamped tightly to prevent interfacial slip. This decreases the damping by the joints to a minimum (6).

The benefits gained by friction damping in joints can no longer be overlooked. The disadvantages can be overcome by improving the surface finish and applying joint damping at selected joints, as opposed to all the joints. Careful selection of joints where friction damping is obtained by slip in rotation, but not in translation, need sacrifice little static stiffness (4). Furthermore, conservative results may be obtained by linear analysis (5). Therefore, it may be feasible to increase the inherent damping in a structure by allowing more friction damping than is presently allowed, thereby controlling the vibration response. This technique can help to avoid complex, active damping systems. Some of the advantages would be lower cost, achievement of high damping, the ability to move resonant frequencies, and the ability to use existing joints (5).

1.2 PURPOSE

The purpose of this thesis was to investigate frictional damping effects in a beam with a rotational joint. The major thrust of this effort was to take an existing finite element computer program, FEM1D (15), and apply friction damping to change the vibration response of the physical model and thereby show the capability to control the vibration response and resonant frequency.

1.3 General Approach and Assumptions

The structure that presented itself most readily to serve as a physical model for this study was a two element beam clamped at both ends with a joint located at the middle node of the beam. A sketch of this set-up is shown in Fig. 1.1a. In the static case, when the beam was subjected to a vertical load at the midpoint, the beam would deflect and a moment would build at the joint due to a frictional moment opposing slip and forcing the slope to remain fixed at zero. When the moment reached the value of the friction moment, any further increase of load would cause the joint to slip and an energy loss would be realized due to the relative

rotation of the two interfaces. A new displacement and slope would be obtained, different from those of the totally locked joint and the value of the moment at the joint would equal the friction moment value. Figs. 1.1b and c, show respectively the cases where the moment is less than the friction moment and when the beam slips because additional load is applied once the friction moment is reached. In the dynamic case, the loss of energy due to slip would be seen as a decrease in the amplitude of the vibrating beam from cycle to cycle.

A literature search showed that interest in the field of friction damping in joints has been around for some time. However, there is very limited vibration data available in which friction forces play a significant role (19). The number of variables associated with friction damping made it difficult to predict, so it was avoided. But because of SDI, the number of studies undertaken to predict the effect of friction damping in joints should increase significantly. Through the judicious use of assumptions, the scope of the problem can be narrowed so that a starting point can be obtained.

The ability to predict or control the damping produced by partial slip between surfaces can be accomplished in the laboratory on only very simple systems (14). For this reason, macroslip was assumed for the joint under investigation. In other words, when the joint was slipping, the total contact area would be slipping. This leads to the

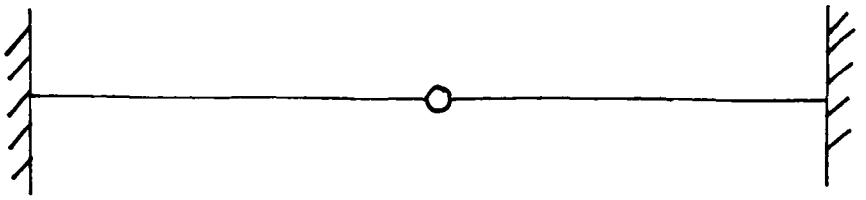

FIGURE 1.1a TWO ELEMENT BEAM MODEL

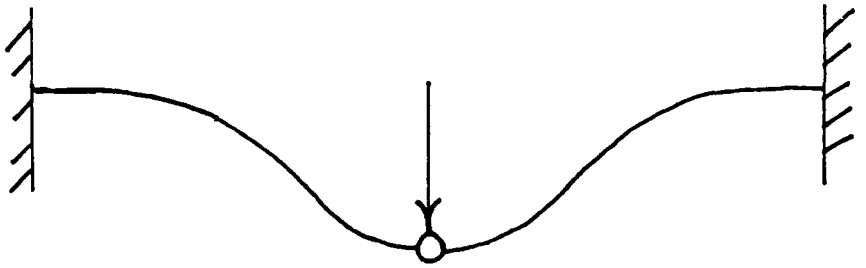

FIGURE 1.1b BEAM WITH M < M_{GROSS}

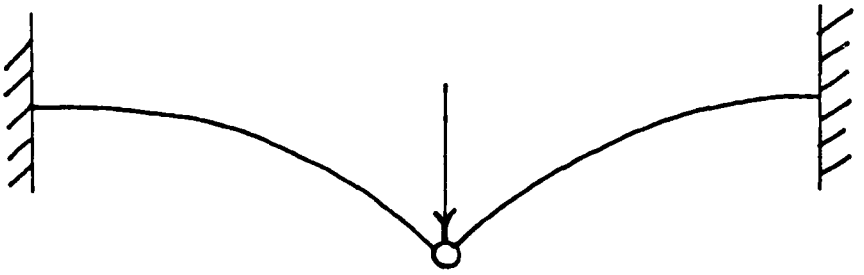

FIGURE 1.1c SLIPPED BEAM

next assumption regarding the clamping pressure.

The clamping pressure was applied such that it was evenly distributed across the contact area. If a bolt is used to apply the clamping pressure, then the pressure is at a maximum near the bolt location and decreases as you go away from it. The area near the bolt would be more rigid and would resist slip more than the outer area. The increased pressure near the bolt would mean that the friction moment would be greater near the bolt. In order to have a constant friction moment across the contact surface, which the macroslip assumption attempted, a uniform clamping pressure was applied. Another asumption was required to insure a constant friction moment.

The friction force applied to the problem is proportional to the clamping pressure through the coefficient of friction, μ. Since the clamping pressure is applied uniformly over the contact area, the coefficient of friction must be constant to provide a constant friction force over the entire area. This assumption of constants also carries over to the time-dependent problem.

Since the solution of a vibrating beam is a time-dependent problem, the clamping pressure and coefficient of friction must be constant in time or the friction force will vary. The first step is to find a solution for the constant friction force or too many variables will be introduced to solve the problem. Hence, the friction force is assumed to be constant with time. This leads us to the physical beam

model.

A simple beam model that is available is the Euler beam. The theory of the Euler beam states that a plane cross-section drawn perpendicular to the centerline of an unbent beam will remain perpendicular to the centerline after the beam bends (9). The Timoshenko beam does not require the cross-section to remain perpendicular to the beam centerline and so more closely approximates the exact beam (9). The dimensions of the clamped-clamped beam were chosen such that the results obtained for the first mode would closely approximate that of the Timoshenko beam. Consequently, the simple thin-beam Euler model will give adequate results for the first mode.

Finally, a modification had to be made to the clamped-clamped beam model. A one-dimensional finite element program was used to model the physical beam and provide the numerical analysis for the dynamics of the beam. The one-dimensional program did not allow for independent rotations of the elements at continuous nodes; it forced the slope at the middle node to remain zero. But for damping to take place, relative rotations had to occur at the node to dissipate energy. So the beam was changed by symmetry about the joint to a cantilever beam with an applied end moment. The slope would be fixed whenever the moment was less than the frictional moment, and would be allowed to change when the value of the moment reached the friction moment value. This allowed the rotations required to calculate energy loss.

CHAPTER 2

THEORY

2.1 Coulomb Damping Theory

Coulomb, or dry friction damping arises whenever two bodies are allowed to slide or rub against one another. For any sliding to take place there must be a force acting which overcomes the resistance caused by friction. The friction force is parallel to the surface and proportional to the force normal to the surface. The classical law of sliding friction states that this frictional force is independent of the contact area and the magnitude of the velocity, as long as sliding exists (9). The friction force opposes the relative motion, and thereby continuously absorbs energy so long as the relative velocity exists. The force of friction is of constant magnitude and as long as the forces acting (namely, the inertia force and the restoring force) are sufficient to overcome the friction force, damping will continue. When the forces become too small, the damping stops as sliding ceases.

This can be illustrated by the motion of the simple spring-mass system of Fig. 2.1.

The mass is set into motion by pulling it in the positive direction and releasing it. The friction force acts in the opposite direction of the velocity of the mass. It is proportional to the force acting normal to the contact

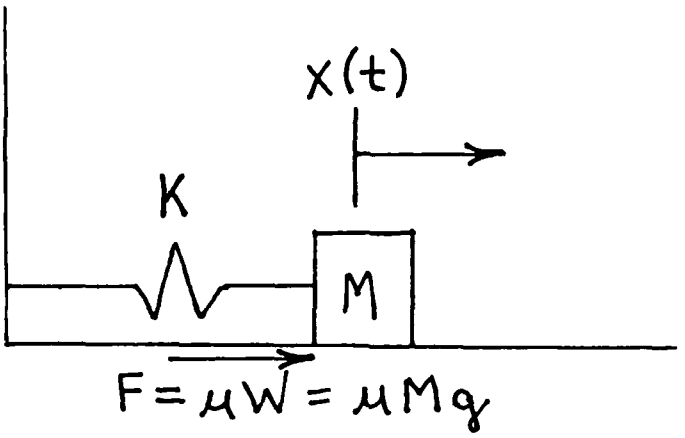

FIGURE 2.1 SIMPLE SPRING-MASS SYSTEM

surface, in this case the weight of the mass. The constant of proportionality is the coefficient of friction, μ. This constant depends only on the roughness of the sliding surfaces. The force of friction is therefore represented by

$$F_d = \mu W = \mu mg \qquad (2\text{-}1)$$

The equation of motion for this system can be written as

$$m\ddot{x} + F_d \mathrm{sgn}(\dot{x}) + kx = 0 \qquad (2\text{-}2)$$

where the symbol "sgn" represents a function having a value of +1 if $\dot{x}$ is positive and -1 if $\dot{x}$ is negative. The equation of motion for this system is non-linear, but it can be separated into two linear equations, one for the positive velocity and one for the negative velocity (12).

$$m\ddot{x} + kx = -F_d \qquad \dot{x} > 0 \qquad (2\text{-}3a)$$

$$m\ddot{x} + kx = F_d \qquad \dot{x} < 0 \qquad (2\text{-}3b)$$

The non-linearity consists of switching between the two linear equations. The switching does not occur as an explicit function of time, but is determined by the

response. Therefore, it could occur at various times, depending on the forcing function and the initial conditions. This means the equation of motion must be solved for one time interval at a time, depending on the sign of $\dot{x}$.

If the mass is displaced initially in the positive direction, the velocity will be negative at first, so the first equation is considered. It can be rewritten in the form

$$\ddot{x} + w_n^2 x = w_n^2 f_d \qquad (2\text{-}4)$$

where $w_n^2 = \frac{k}{m}$ (Natural Frequency of Vibration)

$$f_d = \frac{F_d}{k}$$

The initial conditions are $x(0)=x_o$ and $\dot{x}(0)=0$ so the solution is (12)

$$x(t) = (x_o - f_d)\cos(w_n t) + f_d \qquad (2\text{-}5)$$

This represents harmonic oscillation and is valid for $0 \leq t \leq t_1$, where t_1 is the time at which the velocity reduces to zero and the motion is about to reverse. To find the velocity the equation is differentiated with respect to time to obtain

$$\dot{x}(t) = -w_n(x_o - f_d)\sin(w_n t) \qquad (2\text{-}6)$$

so that the lowest non-trivial solution satisfying the initial condition is $t_1 = \pi/w_n$. If $x(t_1)$ is large enough to overcome the static friction, the mass will have a positive velocity and then must satisfy the other linear equation of

motion. Thus the following equation must be solved

$$\ddot{x} + w_n^2 x = - w_n^2 f_d \qquad (2\text{-}7)$$

with the initial conditions of $x(t_1) = -(x_o - 2f_d)$ and $\dot{x}(t_1)=0$. The solution is (12)

$$x(t) = (x_o - 3f_d)\cos(w_n t) - f_d \qquad (2\text{-}8)$$

This solution is valid for the values of $t_1 \leq t \leq t_2$ where t_2 is the value at which the velocity again goes to zero. The value of t_2 is found to be $2\pi/w_n$. The procedure is then repeated for $t > t_2$, until the motion stops. However, a pattern is seen to emerge.

Over each half-cycle the motion consists of a constant component and a harmonic component with the frequency equal to the natural frequency of the spring-mass system, where the duration of every half-cycle is equal π/w_n. The average value of the solutions switches between f_d and $-f_d$ and at the end of each half-cycle the displacement is reduced by $2f_d = 2\mu mg/k$. This leads to the conclusion that in coulomb damping the amplitude decays linearly with time, not exponentially as in viscous damping (12). A plot showing the decay as a function of time for this simple system is seen in Fig. 2.2. Fig. 2.2 also shows that the curve oscillates about the values of f_d and $-f_d$ and if the restoring force falls below this value, the block will stop sliding at some position on either side of zero, depending on the initial displacement.

One may associate coulomb friction with rotational slip by looking at the force of sliding friction coming from

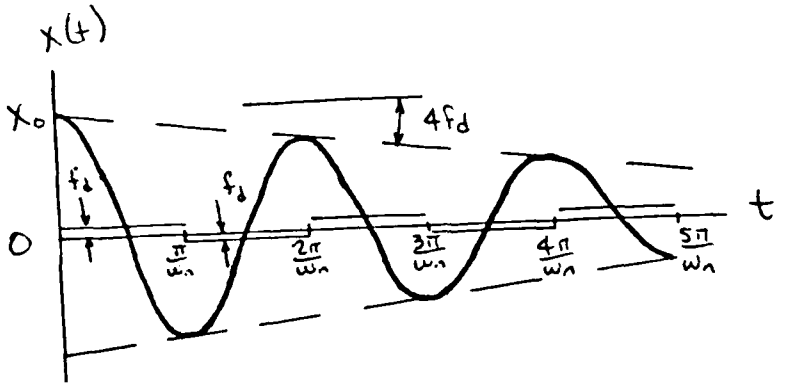

FIGURE 2.2 LINEAR FRICTION DAMPING DECAY (12)

a frictional shear stress at the contact area that is equal to μ times the normal pressure. This gives an equivalent result to the simpler cases, such as the sliding block previously mentioned. This case aids in the solution of more complicated systems, such as curved contact surfaces or non-uniform pressure or velocity distributions (10).

To show this case, assume a frictional moment arises from the flat end of a circular rotating shaft of radius R being pressed against a plane surface with a total force N (10). Also assuming a uniform normal pressure or compressive stress on the contact area A, we obtain a uniform frictional stress of magnitude (10)

$$\tau_f = \mu \frac{N}{A} = \frac{\mu N}{\pi R^2} \qquad (2\text{-}9)$$

which is everywhere in a direction normal to a radial line drawn from the center of the circular contact area. From Fig. 2.3 it is seen that the moment due to an annular

element of width dr and area $2\pi r dr$ is

$$dM = \tau_f 2\pi r^2 dr = \frac{\mu N}{\pi R^2} 2\pi r^2 dr \qquad (2\text{-}10)$$

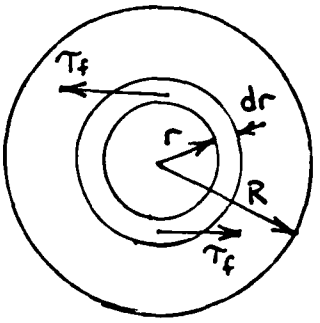

FIGURE 2.3 FRICTION STRESS ON ROTATING CIRCULAR SURFACE (16)

The total frictional moment is

$$M = \frac{2\mu N}{\pi R^2}\int_0^R r^2 dr = \frac{2}{3}\mu NR \qquad (2\text{-}11)$$

If $\mu = 0$, the contact surface is said to be perfectly smooth. If, on the other hand, $\mu = \infty$, a perfectly rough surface exists. The first case corresponds to the no clamp case in which the friction force is zero. The second case corresponds to the relative velocity at the point of contact being zero and is referred to as the no slip case (10).

As an extension to this case, Richardson and Nolle assumed that an external moment applied to a rotary joint is transferred between the two surfaces by shear due to friction (16). Fig 2.4 depicts the transfer at the friction

interface. Also, the friction shear stress is considered constant and occurs only in those regions of the contact surface where relative slip occurs (16). As the

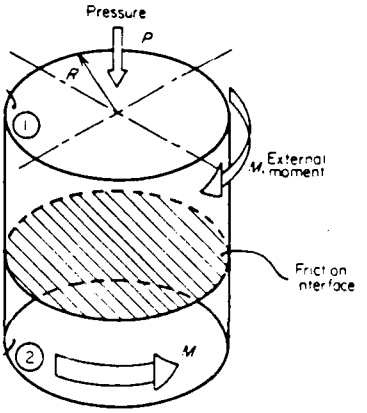

FIGURE 2.4 TRANSFER OF MOMENT BY SHEAR DUE TO FRICTION (15)

applied moment is increased, slip begins at the outer edge of the contact circle and extends inward to a constant restoring moment. Fig. 2.5 shows the slipped region for a particular applied moment.

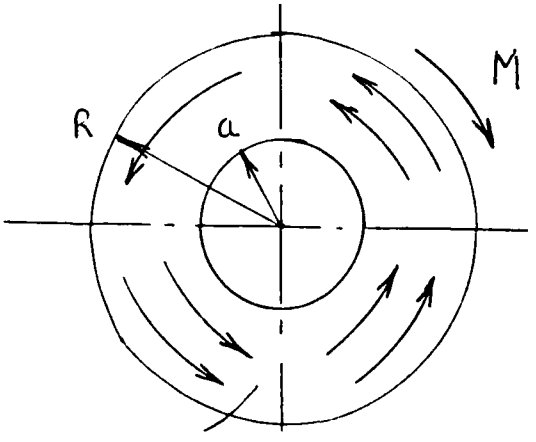

FIGURE 2.5 SLIPPED REGION/DISTRIBUTION OF SHEAR STRESSES(16)

The moment is applied from zero to a value of M_{MAX}.

The inner bounding radius can be calculated from equilibrium of moments.

$$M = \int_a^R 2\pi r^2 \mu P dr \qquad \text{yields} \qquad a^3 = R^3 - 3M/2\pi\mu P \qquad (2\text{-}12)$$

where P = Clamping Pressure

For gross sliding, the slipped region covers the entire contact area (a = 0), so the moment for gross slip to occur is

$$M_{GROSS} = 2\pi\mu PR^3/3 \qquad (2\text{-}13)$$

For any applied moment below M_{GROSS} the relative slip is in the microslip stage. At M_{GROSS}, macroslip would be said to to occur. The value of M_{GROSS} can be varied as a function of clamping pressure. The low end of the macroslip region occurs at low clamping forces and is known as the no-clamp case. As the moment increases to M_{GROSS}, the amount of damping increases until M_{GROSS} is reached. Above M_{GROSS}, damping decreases in the microslip region until the clamping

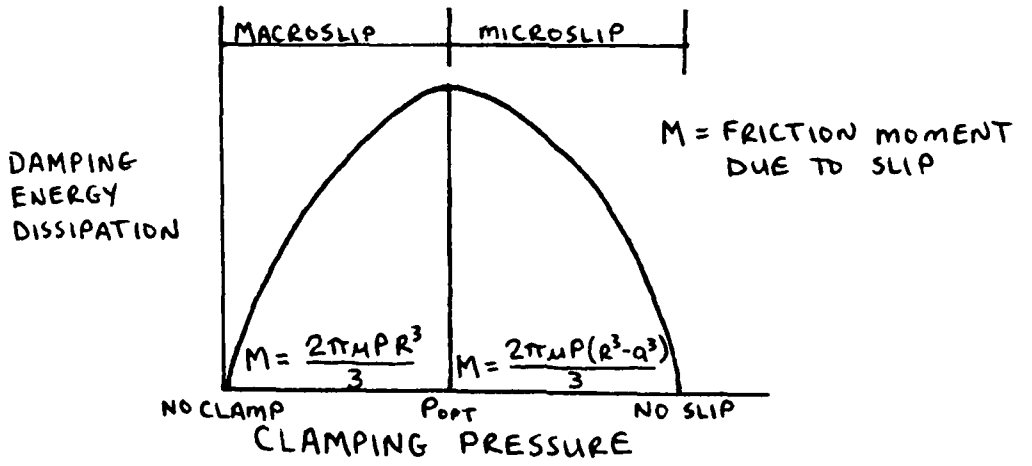

FIGURE 2.6 DAMPING VS CLAMPING PRESSURE (11)

pressure is so great that no relative slip occurs. This is the no-slip case. Lazan shows the relationship between damping and clamping pressure graphically in Fig. 2.6 Damping is maximized at some clamping pressure just above that required to prevent gross slip (21). This is because the entire surface undergoes slip and no more damping can take place than when the friction moment is at a maximum.

2.2 Thin Beam Theory vs the Timoshenko Beam

Thin beam theory states that a cross-section perpendicular to the beam axis prior to beam bending will remain perpendicular to that axis after the beam bends (9). The

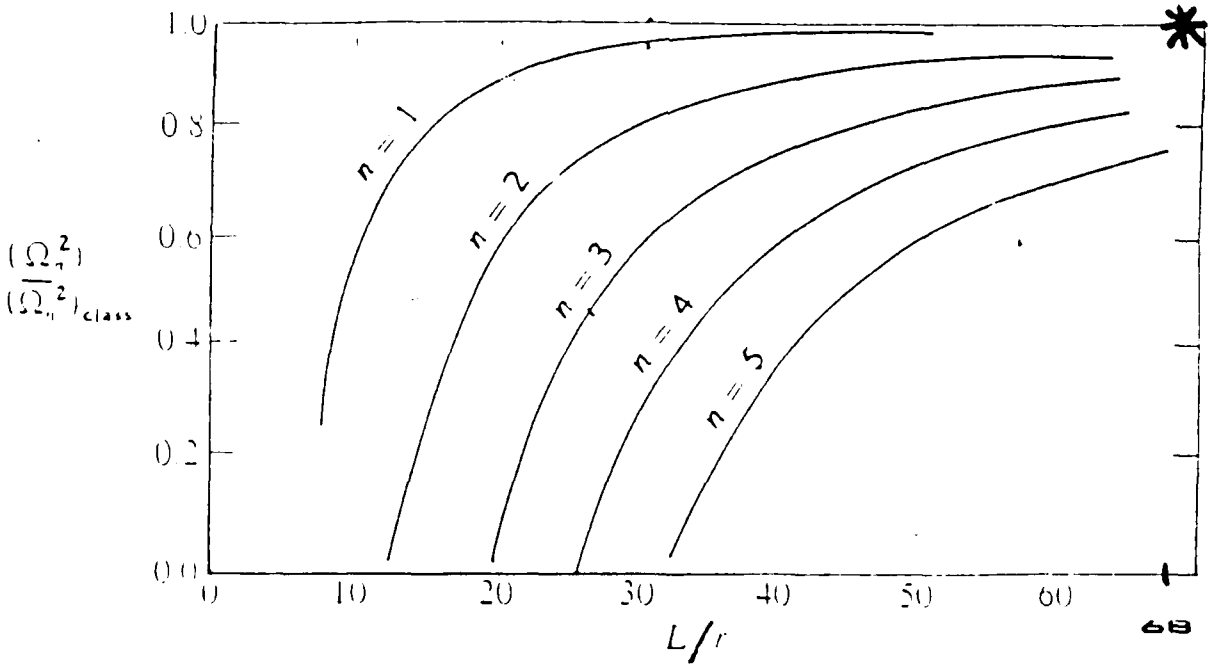

$$\frac{\text{LENGTH}}{\text{RADIUS OF GYRATION}} = \frac{L}{\sqrt{\frac{I}{A}}} = \frac{L}{\sqrt{\frac{bh^3}{12bh}}} = \sqrt{12}\,\frac{L}{h}$$

FIGURE 2.7 TIMOSHENKO BEAM VS THIN BEAM (9)

Timoshenko beam does not require this to happen and therefore models the real beam better. In an effort to estimate the amount of error thin beam theory would enter into the problem, it was compared to Timoshenko theory. Fig. 2.7 compares a non-dimensional frequency for the Timoshenko beam vs the classical beam (thin beam). The length to height of the physical beam model gives an L/r value of 68. This compares quite well with the Timoshenko beam for the first mode, as shown by the * in Fig. 2.7. Errors may show-up for higher vibration modes, but the thin-beam theory will be adequate for predicting the first vibration mode.

2.3 Finite Element Theory for Time-Dependent Problems

In time-dependent problems, the undetermined parameters are assumed to be functions of time and the approximation functions are assumed to be functions of spatial coordinates. Two stages of solution must be undertaken, both involving approximate methods. First, the spatial approximation must be considered and then the time approximation. This procedure is known as semidiscrete approximation (in space) (15). The spatial approximation leads to a set of ordinary differential equations in time. In structural dynamics, these equations quite often contain second-order time derivatives of the dependent variables. The spatial approximation forms the equations of motion in

matrix form as

$$[M]\{\ddot{x}\} + [K]\{x\} = \{F\} \qquad 0 < t < t_o \qquad (2\text{-}14)$$

where [M] = mass matrix

[K] = stiffness martix

{x} = displacement vector

{F} = applied loads vector

This equation must be further approximated to get a set of algebraic equations which can then be solved. There are several schemes available for solving the above equation. The most common one is the Newmark-Beta direct integration method (15). The Newmark-Beta method approximates the first time derivative $\{\dot{x}\}$ and the function {x}, which is time dependent, at the (n + 1)st time step (Δt= constant) as(15)

$$\{\dot{x}\}_{n+1} = \{\dot{x}\}_n + [(1-\gamma)\{\ddot{x}\}_n + \gamma\{\ddot{x}\}_{n+1}]\Delta t \qquad (2\text{-}15a)$$

$$\{x\}_{n+1} = \{x\}_n + \{\dot{x}\}_n\Delta t + [(\tfrac{1}{2} - \beta)\{\ddot{x}\}_n + \beta\{\ddot{x}\}_{n+1}](\Delta t)^2 \qquad (2\text{-}15b)$$

where γ and β control the accuracy and stability of the scheme and subscript n shows that the solution is computed at time $t = t_n$. The values of $\gamma = \frac{1}{2}$ and $\beta = \frac{1}{4}$ are normally chosen because they provide for an unconditionally stable system. This means that the size of the time step is goverened by the need for accuracy rather than stability. This scheme, known as the constant average acceleration method (15), is very valuable in computing the response of systems in which damping is introduced externally because the method itself does not introduce any damping. Equations (2-14) and (2-15) can be combined and rearranged to get (15)

$$[\hat{K}]\{x\}_{n+1} = \{\hat{F}\}_{n+1} \qquad (2\text{-}16)$$

where $\hat{[K]} = [K] + a_0[M]$

$$\hat{\{F\}}_{n+1} = \{F\}_{n+1} + [M](a_0\{x\}_n + a_1\dot{\{x\}}_n + a_2\ddot{\{x\}}_n)$$

Given initial conditions of $\{x\}_0$, $\dot{\{x\}}_0$, and $\ddot{\{x\}}_0$, equation (2.16) can be solved repeatedly for $\{x\}$. If the initial value of the acceleration is not given, which is usually the case, equation (2-14) can be used to compute $\ddot{\{x\}}$ at t = 0. After calculating $\{x\}$ at $t_{n+1} = (n+1)\Delta t$, the first and second derivatives (velocity and acceleration) of $\{x\}$ at t_{n+1} can be found by rearranging equation (2-15) (15)

$$\ddot{\{x\}}_{n+1} = a_0(\{x\}_{n+1} - \{x\}_n) - a_1\dot{\{x\}}_n - a_2\ddot{\{x\}}_n \qquad (2\text{-}17a)$$

$$\dot{\{x\}}_{n+1} = \{x\}_n + a_3\ddot{\{x\}}_n + a_4\ddot{\{x\}}_{n+1} \qquad (2\text{-}17b)$$

where $a_0 = 1/[\beta(\Delta t)^2]$ $\quad a_1 = a_0\Delta t$ $\quad a_2 = (1/2\beta) - 1$

$a_3 = (1 - \gamma)\Delta t$ $\quad a_4 = \gamma\Delta t$

Given initial conditions of $\{x\}_0$, $\{x\}_0$, and $\{x\}_0$, equation (2.16) can be solved repeatedly for $\{x\}$ and its time derivatives at any time $t > 0$.

Newmark-Beta is unconditionally stable, as previously mentioned, which means the solution does not grow without limit. However, if the right time step is not chosen the results may be inaccurate. An estimation for the time step is given by (15)

$$\Delta t = T_{min}/\pi \qquad (2\text{-}18)$$

where T_{min} is the smallest period of vibration given by the problem. This assures not only a stable solution for any Δt but also accuracy of results. The smallest period in the clamped-clamped beam occurs when the joint is fully clamped. The period was obtained from the unmodified FEM1D program.

The value was 0.0074074 sec. Substituting this number into Eqn. (2-18), a Δt of 0.0023579 was computed. Therefore, any value of Δt below this number would guarantee accuracy of results. The value of $\Delta t = 0.0001$ was chosen for calculation in the Newmark Beta method in an effort to obtain increased accuracy.

Fig. 2.8 highlights the main steps of the Newmark Beta time integration method. Fig. 2.9 compares the accuracy of the Newmark Beta method with other numerical analysis methods and the exact solution. The problem being solved in Fig. 2.9 is a two element axial rod clamped at one end. The top plot shows the axial displacement of the middle node and the bottom plot shows the axial displacement of the node at the free end. Notice that while the other numerical methods display some form of amplitude decay, the Newmark Beta method does not. However, Newmark Beta does exhibit some period elongation, and this should be considered if accurate frequency calculations are required.

FIGURE 2.8 NEWMARK BETA INTEGRATION METHOD

A. Initial Calculations

1. Form K, and M.

2. Initialize x_o, $\dot{x}_o$, and $\ddot{x}_o$.

3. Select time step Δt, γ and β ($\gamma \geq \frac{1}{2}$, $\beta \geq \frac{1}{4}(0.5 + \gamma)^2$), and calculate :

$$a_0 = 1/(\beta \Delta t^2) \; ; \; a_1 = 1/(\beta \Delta t) \; ; \; a_2 = (1/2\beta) - 1$$

$$a_3 = \Delta t(1-\gamma) \; ; \; a_4 = \gamma \Delta t$$

4. Form the matrix $\hat{K} = K + a_0 M$.

B. For each time step

1. Calculate the effective loads at time $t + \Delta t$:

$$\hat{F}_{t+\Delta t} = F_{t+\Delta t} + M(a_0 x_t + a_2 \dot{x}_t + a_3 \ddot{x}_t)$$

2. Solve for the displacements at $t + \Delta t$:

$$\hat{K} x_{t+\Delta t} = \hat{F}_{t+\Delta t}$$

3. Calculate the accelerations and velocities at $t + \Delta t$:

$$\ddot{x}_{t+\Delta t} = a_0(x_{t+\Delta t} - x_t) - a_1 \dot{x}_t - a_2 \ddot{x}_t$$

$$\dot{x}_{t+\Delta t} = \dot{x}_t + a_3 \ddot{x}_t + a_4 \ddot{x}_{t+\Delta t}$$

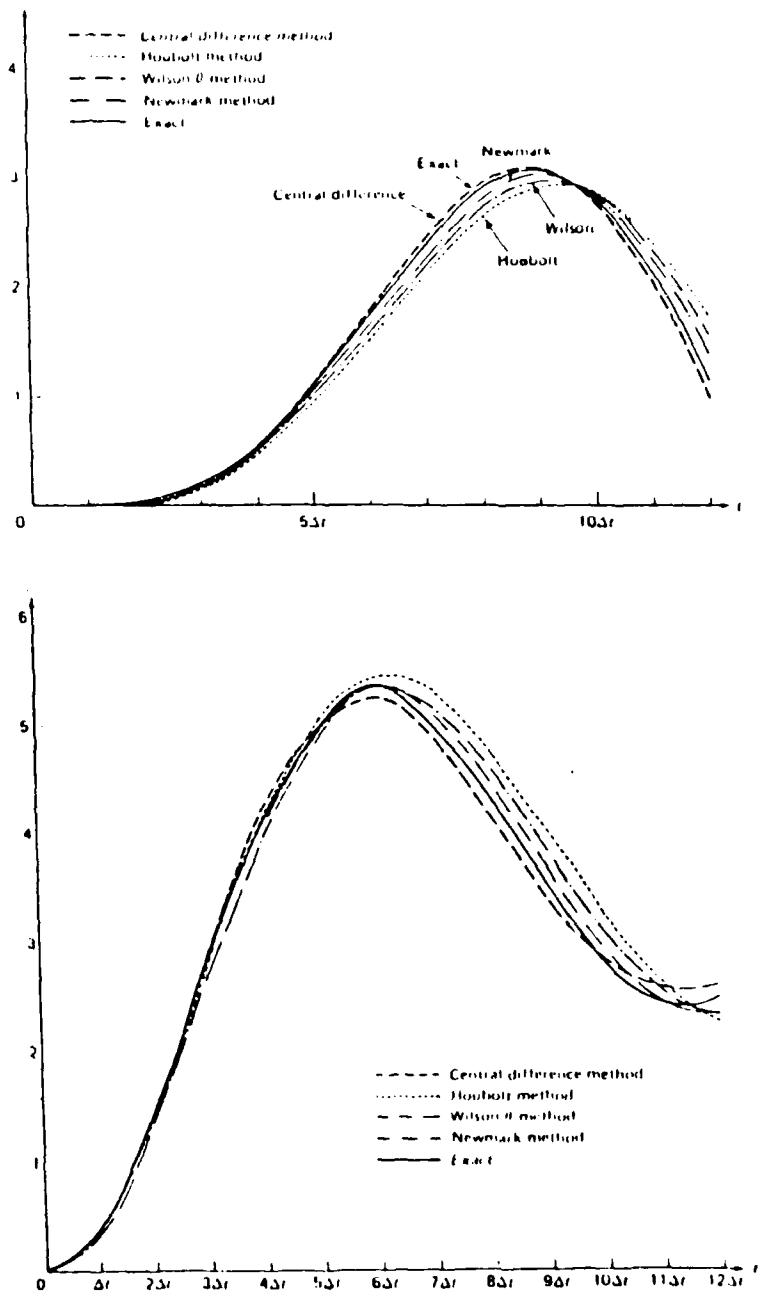

FIGURE 2.9 Newmark Beta vs. Other Numerical Methods(22)

CHAPTER 3

THE DAMPING MODEL

3.1 THE BEAM IN STATIC BENDING

The physical dimensions of the two element beam arrangement can be seen in Fig. 3.1. However, because of the limitations of the FEM1D computer program, the actual beam model that was used in the computer analysis was a cantilever beam with an applied end moment. The beam was made of steel; the material properties and related calculations to be used in the computer analysis can be found in Appendix 1.

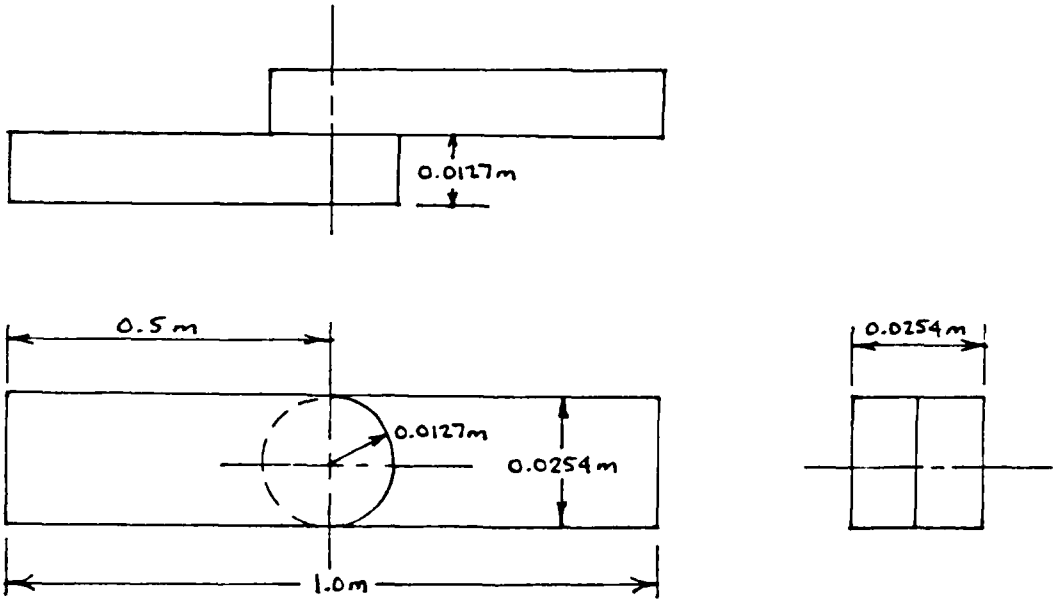

FIGURE 3.1 PHYSICAL BEAM DIMENSIONS

The computer program allowed certain boundary conditions to be fixed, so initially it was assumed that no slip would take place and the slope at the tip was fixed at

zero. As a vertical load was applied, a moment was generated to keep the slope fixed at zero. If the value of M_{GROSS} was not equaled, then no slip took place and the beam would behave as a normal clamped-clamped beam in bending. When the value of the moment reached the value of MGROSS, the next increment of load would cause the joint to slip because, due to friction, the joint cannot hold any more moment than the value of M_{GROSS}. At this point, the boundary conditions were changed and the restriction that the slope remain zero was removed. A moment equal to the value of M_{GROSS} was applied opposite to the direction of impending motion, and slip occured due to the change in slope. A new value of displacement and slope were found, different than the value for the clamped-clamped beam. Fig. 3.2 shows the shape of the beam and equation that is solved for the static beam where the moment does not equal M_{GROSS}.

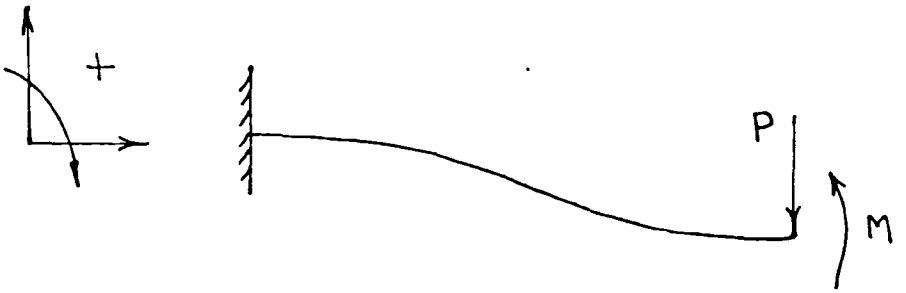

$$[K]\begin{Bmatrix} w \\ \theta \end{Bmatrix} = \begin{Bmatrix} P \\ M \end{Bmatrix}$$

FIGURE 3.2 UNSLIPPED STATIC BEAM

Once slip occurred, a new equation was solved because of the boundary condition change. This is seen in Fig. 3.3.

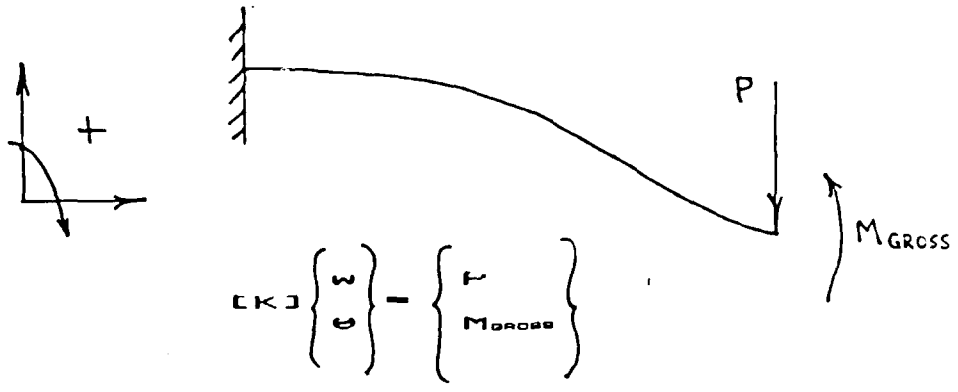

FIGURE 3.3 SLIPPED STATIC BEAM

The solution of the beam in either case can be verified by superpositon once the value of the moment is known. The equations of superposition for beam bending by an applied load and moment at the tip of a cantilever beam are (7)

$$w = -\frac{PL^3}{3EI} + \frac{ML^2}{2EI} \quad \text{AND} \quad \theta = \frac{PL^2}{2EI} - \frac{ML}{EI} \qquad (3\text{-}1)$$

where w = displacement

θ = slope

P = applied load

M = applied moment

L = length

E = modulus of elasticity

I = moment of inertia

3.2 THE BEAM IN DYNAMIC BENDING

Once the static solution was found, the displacement vector was used as initial conditions for a dynamic problem. The initial boundary conditions are such that the slope is

fixed at the value calculated from the static problem. The beam is then set into motion by removing the initial vertical load. The beam begins to move with some velocity, $\dot{w}_2$ (see Fig. 3.4). Initially, the moment that was held at the joint, the value of M_{GROSS}, is relaxed because of load removal. However because the slope is not allowed to change the moment begins to build again. The following differential equation now applies

$$M\ddot{x} + Kx = F \qquad (3\text{-}2)$$

where M = global mass matrix

K = global stiffness matrix

F = applied loads ($F = \{ 0, 0 \}^T$)

Remember that the static equation was just

$$Kx = F \qquad (3\text{-}3)$$

The motion of the beam requires the inclusion of the acceleration terms in the problem. This presents two new terms in the calculation of the moment to compare against M_{GROSS}. The moment calculated was therefore

$$M = M_{43}\ddot{w}_2 + M_{44}\ddot{\theta}_2 + K_{43}w_2 + K_{44}\theta_2 \qquad (3\text{-}4)$$

where the displacement and acceleration vectors are obtained by solving Eqn.(3-2) by the Newmark Beta method. Appendix 2 shows how the boundary conditions are applied to determine which terms will appear in the dynamic moment calculation. Now when this moment equals the value of M_{GROSS}, slip will occur with the next incremental increase in the moment. It can be seen that initially $\ddot{\theta}_2$ is zero, but after slip occurs an angular acceleration term will appear and figure into the

moment equation. The new equation that must be solved once slip occurs is

$$M\ddot{x} + Kx = F \qquad (3\text{-}5)$$

where F = applied loads ($F = \{ 0, M_{GROSS} \}'$).

Fig. 3.4 shows the conditions that exist once slip occurs.

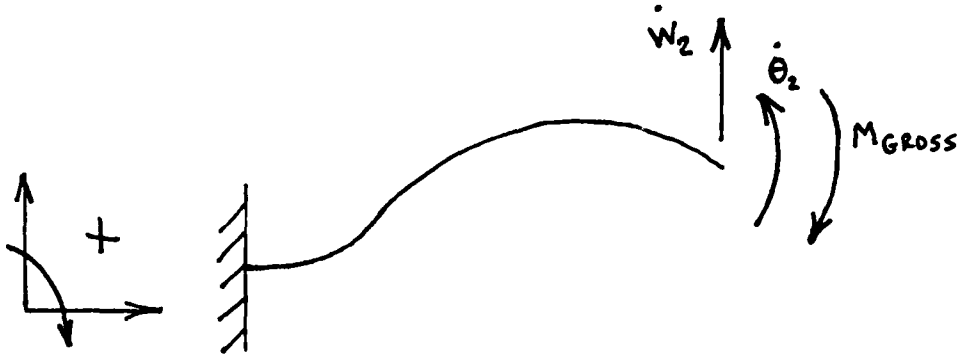

FIGURE 3.4 DYNAMIC BEAM WITH $\dot{\theta}_2 < 0$

Once the slip mechanism is turned on, some method must be available to turn it off. In friction damping the friction force acts opposite the direction of motion of the system. In this case the motion is rotational, so the friction moment opposes the angular velocity of the joint. Therefore, the angular velocity should play some part in monitoring when slip at the joint had stopped. When slip ceases, the angular velocity should be equal to zero. At this point, the slope was fixed and the friction moment removed. The beam would then begin to move in the opposite direction and the process would begin again. Fig. 3.5 shows this case. The moment at this point is positive, but it decreases with time until it becomes negative. When the absolute value of the moment on this stroke equaled the

value of M_{GROSS}, the slope was allowed to change and the friction moment was applied in the opposite direction of the motion. This is illustrated by Fig. 3.6. The process would continue until the moment no longer equalled the value of M_{GROSS} and the beam would oscillate from then on with some permanent slope. Fig. 3.7 shows the logic implemented to solve for the damping at the joint of a vibrating beam. The major modifications were made in the STRESS subroutine of the FEM1D program (15). The actual Fortran code for this subroutine can be seen in Appendix 3.

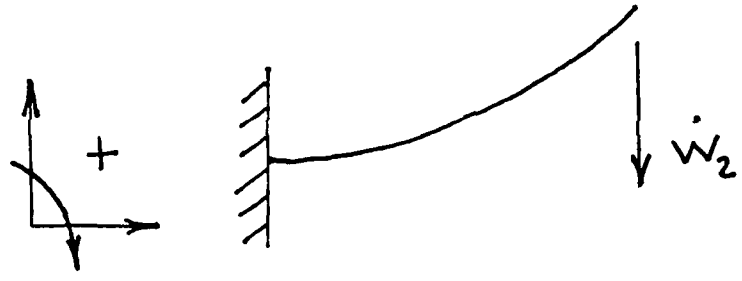

FIGURE 3.5 DYNAMIC BEAM WITH $\dot{\theta}_2 = 0$

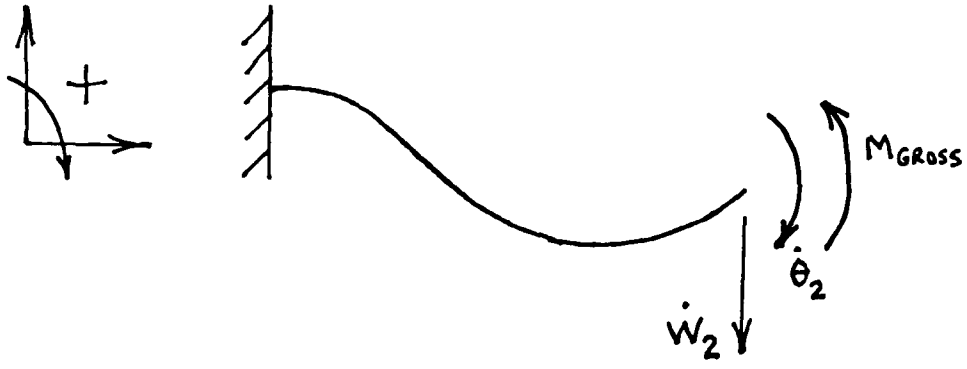

FIGURE 3.6 DYNAMIC BEAM WITH $\dot{\theta}_2 > 0$

FIGURE 3.7 LOGIC OF THE FRICTION DAMPING MECHANISM

For the initial loading of Fig. 1.1c, the flow of the damping mechanism would be:

A. For each time step when not slipping

1. Calculate M_{GROSS}

$$M_{GROSS} = 2\pi\mu PR^3/3 = \text{Constant}$$

2. Calculate M

$$M = M_{43}\ddot{W}_2 + M_{44}\ddot{\theta}_2 + K_{43}W_2 + K_{44}\theta_2$$

3. Compare M vs M_{GROSS}

a. If $|M| \leq M_{GROSS}$ Go on to next time step

b. If $|M| > M_{GROSS}$

1. Remove fixed slope condition

2. Apply tip moment equal to:

a. M_{GROSS} if $M > 0$

b. $-M_{GROSS}$ if $M < 0$

3. Go on to next time step in part B.

B. For each time step that slip is occurring

1. $|M| \approx M_{GROSS}$

2. Check angular velocity, $\dot{\theta}_2$

a. If $M > 0$

1. If $\dot{\theta}_2 < 0$ Go on to next time step

2. If $\dot{\theta}_2 \geq 0$

a. Fix slope at present value (θ_2 = Constant)

b. Remove tip moment

c. Go on to next time step in part A.

b. If $M < 0$

1. If $\dot{\theta}_2 > 0$ Go on to next time step

2. If $\dot{\theta}_2 \leq 0$

a. Fix slope at present value (θ_2 = Constant)

b. Remove tip moment

c. Go on to next time step in part A.

CHAPTER 4

RESULTS

4.1 THE STATIC BEAM

The response of the static beam in bending was readily calculated once the friction moment was obtained. The method consisted of applying superposition when the value of M_{GROSS} was reached. The applied load and moment would then give a displacement and slope at the end node. The values for the the static problem were used as the initial displacement vector for the dynamic problem. Since this is where the interest lies, emphasis is placed on the results of the vibrating beam.

4.2 THE DYNAMIC BEAM

The beam was set into motion with the slope at the joint fixed by removing the initial load. When the dynamic moment reached the value of M_{GROSS}, the boundary condition that kept the slope fixed was removed and a friction moment equal to the value of M_{GROSS} was applied in opposition to the value of the angular velocity. The joint was allowed to slip until the angular velocity reached zero. Then the slope was fixed at the value it had reached at that time and the moment was removed. This process continued until the slope remained fixed continuously and no more slip took place. The values that were deemed important were displacement, slope, and angular velocity. All three of these quantities were plotted versus time to determine how the beam model was responding as a function of time. Figs.

4.1 through 4.4 are plots of the translational displacements versus time for various clamping pressures. Note how the maximum displacement decreases as the clamping pressure increases for an initial applied load of 10,000 N. The maximum displacement occurs at zero clamping pressure and the minimum at the fully clamped case. At low clamping pressures, damping takes place over a longer time period because of the small value of M_{GROSS}, while at the higher clamping pressures, damping takes place for only one or two half-cycles.

Figs. 4.5 and 4.6 show plots of slope at the joint versus time for two clamping pressures. At the lower clamping pressure, the slope was seen to level off periodically and then continue after it had been fixed for a few time steps. This was confusing until the angular velocity versus time plots were examined. These plots are shown in Figs. 4.7 to 4.9.

The angular velocity versus time plot for zero clamping pressure, Fig 4.7, exhibited an unexpected response. Note that a high frequency response is superimposed on a lower frequency. It was determined that two modes of vibration were showing on this plot. The lower frequency trace was the first mode of the beam and the higher frequency in between was the second mode due to the rotation of the end of the beam. When the clamping presure was increased to 8.0E06 N/m^2, both modes were seen to damp out, as would be expected. The higher frequency second mode

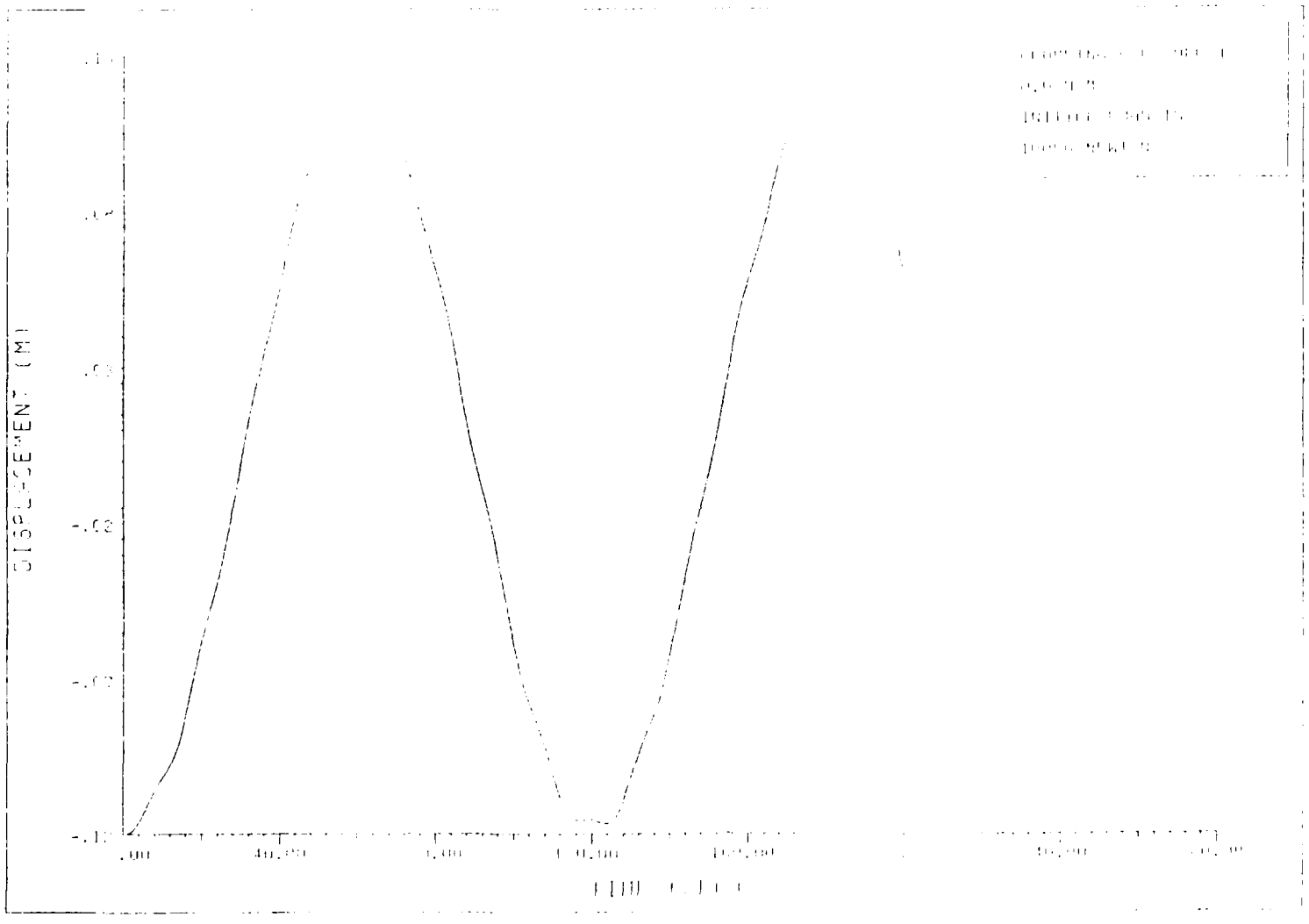

FIGURE 4.1 w_2 vs. Time

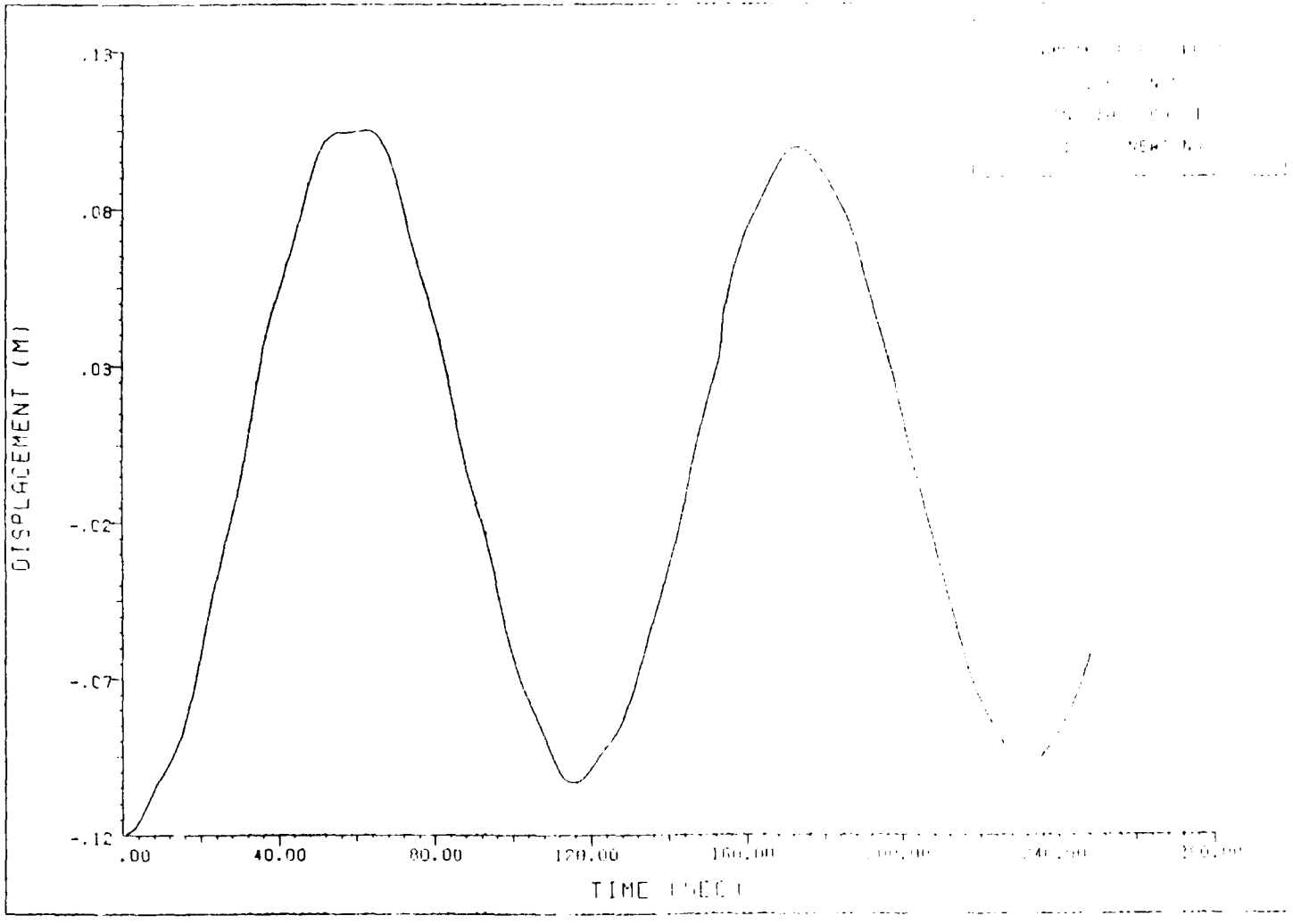

FIGURE 4.2 w_2 vs. Time

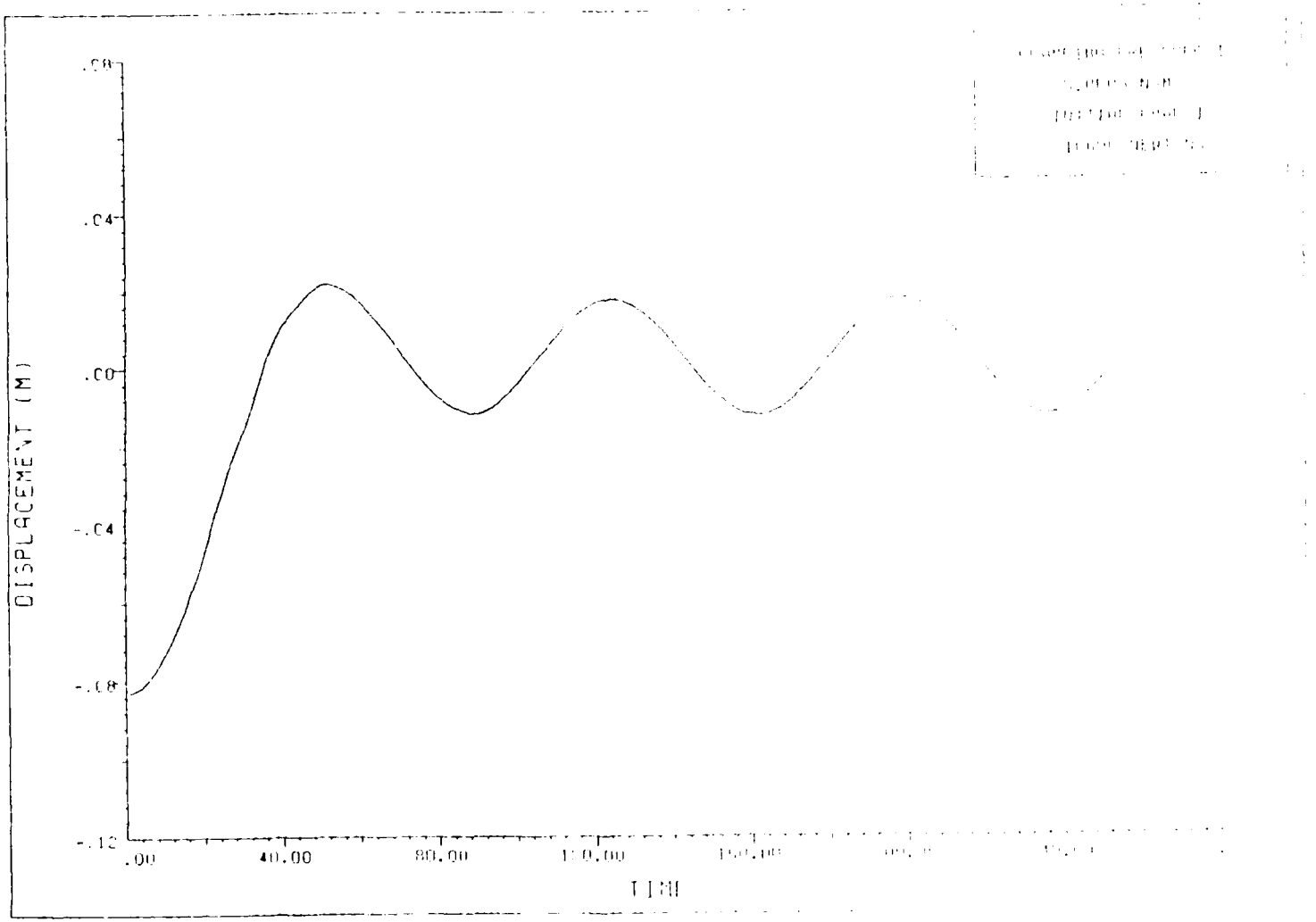

FIGURE 4.3 w_2 vs. Time

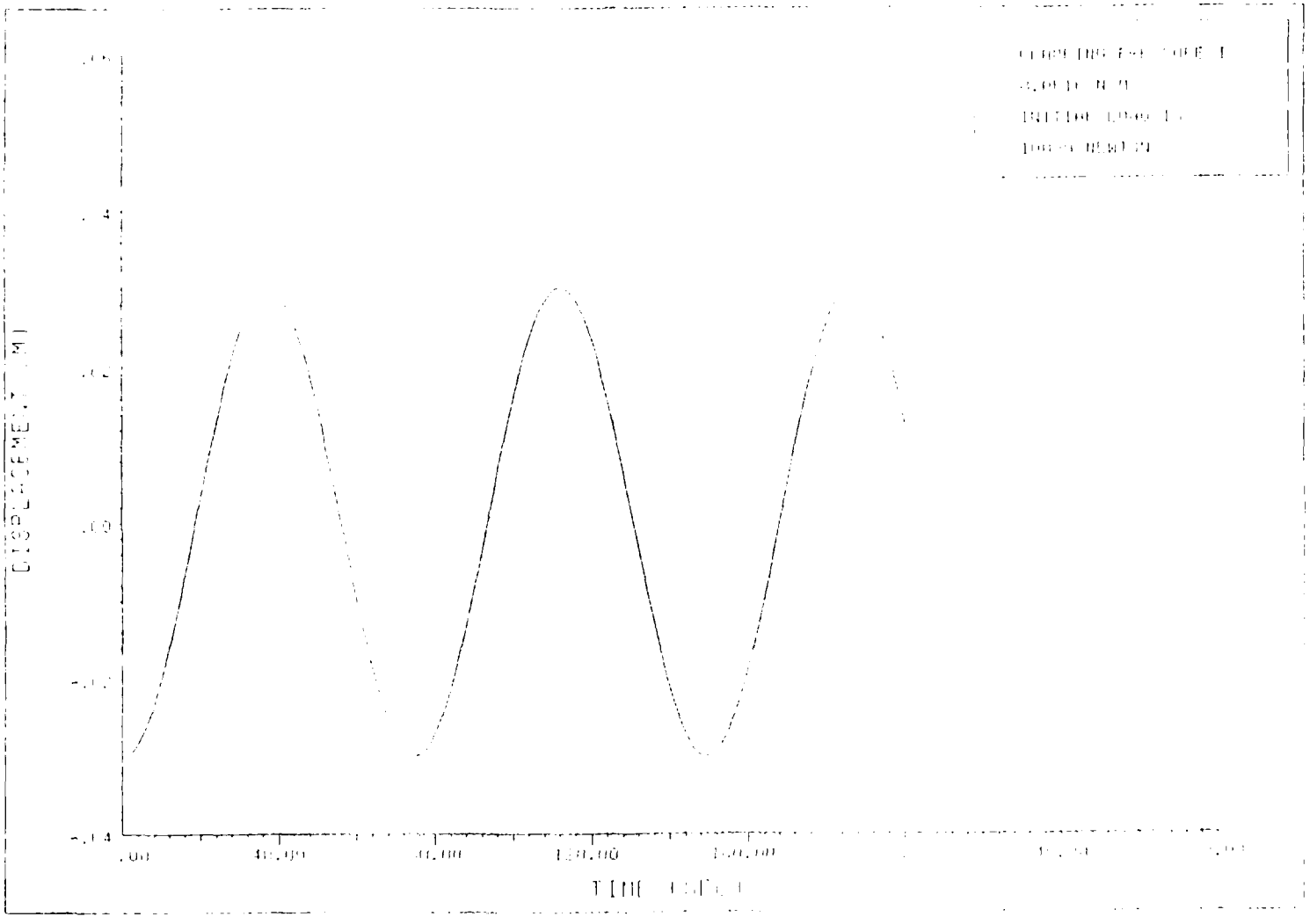

FIGURE 4.4 w_2 vs. Time

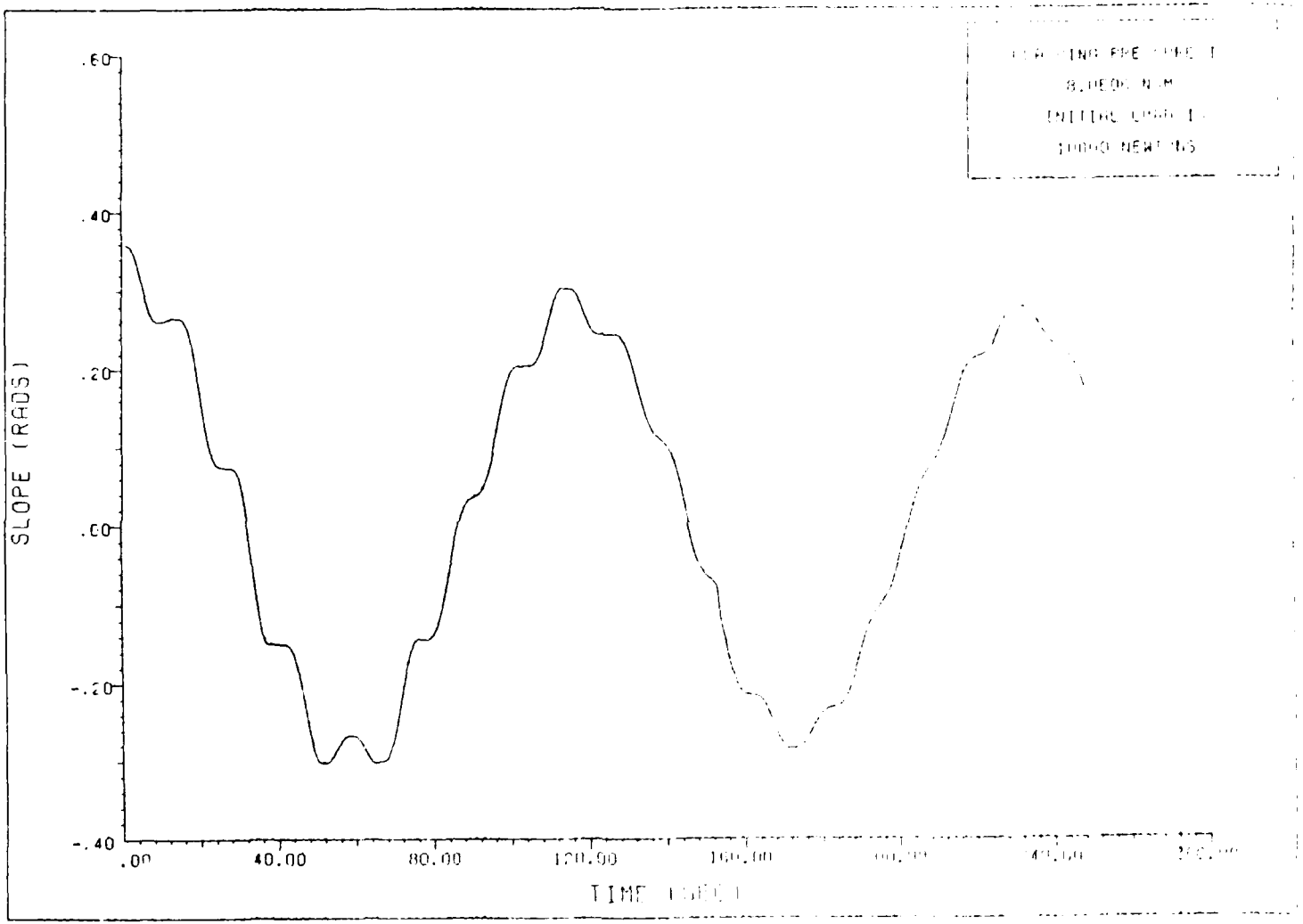

FIGURE 4.5 Slope vs. Time

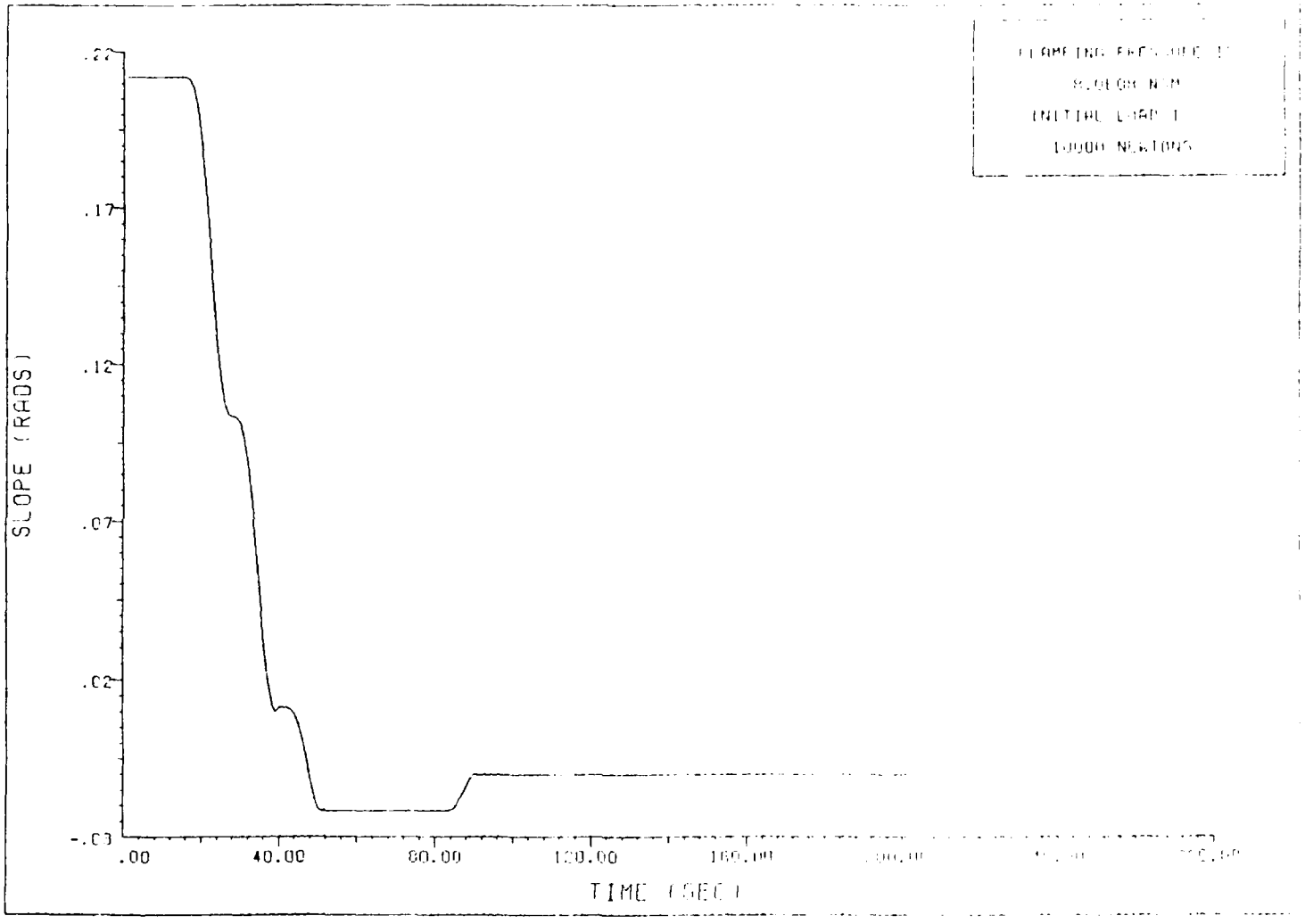

FIGURE 4.6 Slope vs. Time

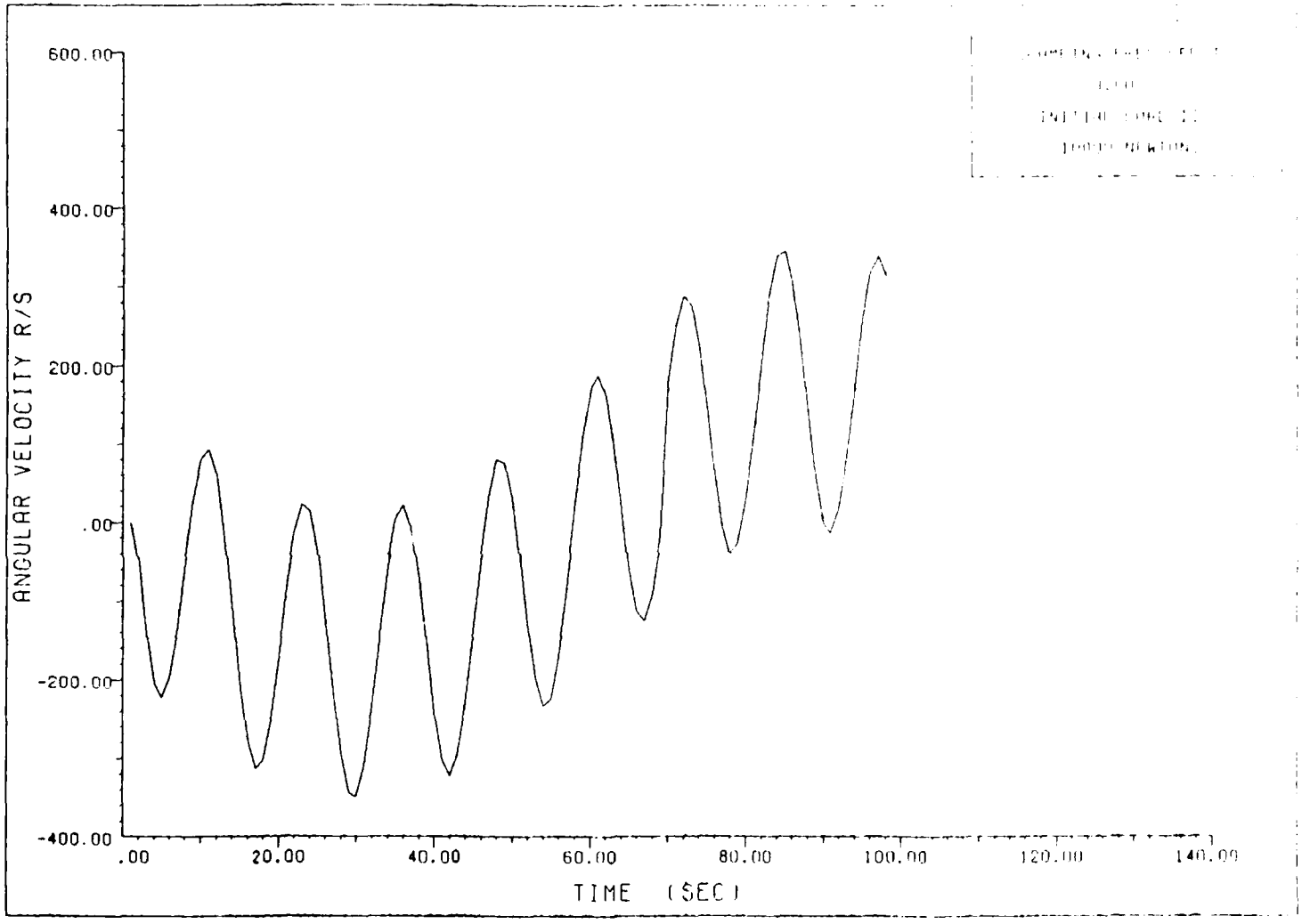

FIGURE 4.7 Angular Velocity vs. Time

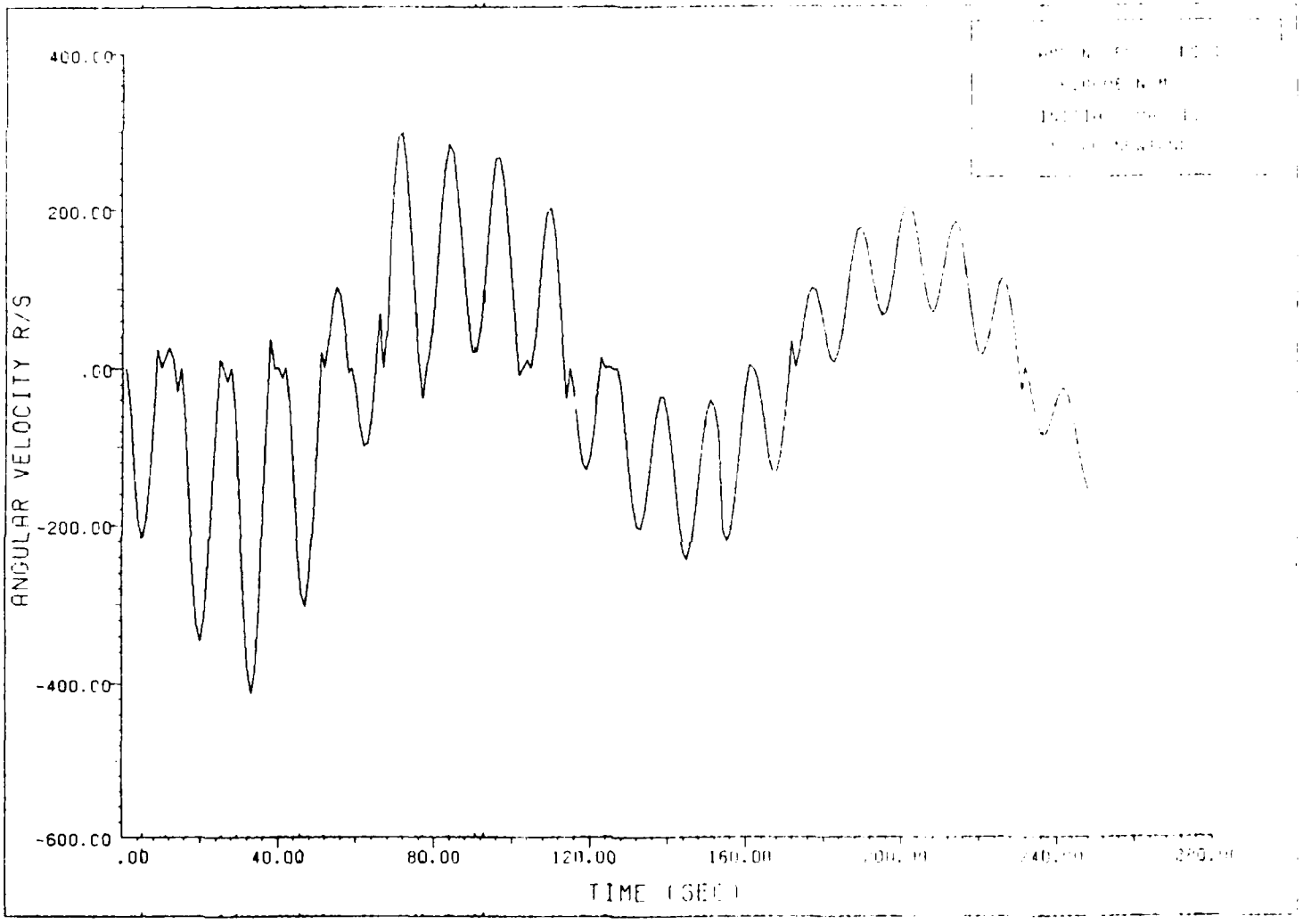

FIGURE 4.8 Angular Velocity vs. Time

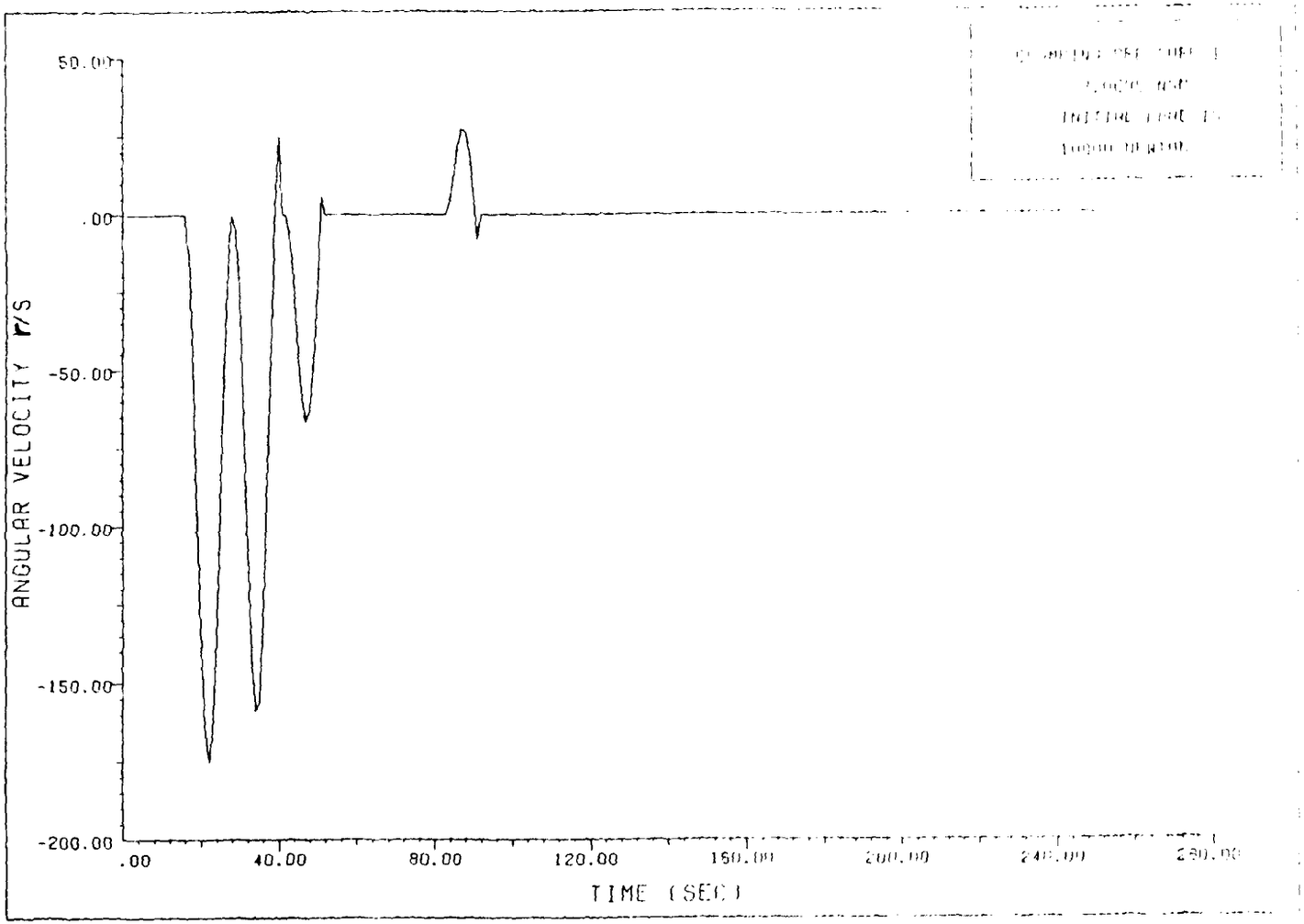

FIGURE 4.9 Angular Velocity vs. Time

damped out first, and the first mode then continued on because there was no structural or viscous damping modelled.

Frequency was plotted as a function of clamping pressure and the lower clamping pressures gave lower frequencies. As the clamping pressure was increased, the beam became more stiff, and so the frequency increased. This is seen in Fig. 4.10. Note that the range of frequencies is bracketted by the values obtained for a cantilevered beam at the low end and a fully clamped beam at the high end.

The slope at which the joint finally locks up, the permanent set, is a function of the initial load and the clamping pressure. It can lock up at a positive or negative slope. Figs. 4.11 through 4.13 depict w_2, θ_2, and $\dot{\theta}_2$ versus time respectively for an initial load of 10,000 N and a clamping pressure of 9.5E08 N/m^2. The permanent set, which was a negative slope for most of the previous runs, is now set at a positve slope. The same effect could have been achieved for a constant clamping pressure and varying initial load. The beam then oscillates about some equilibrium point other than zero. The equilibrium point could also be either positive or negative, again based on the initial conditions.

The shape of the beam was plotted as a function of time. Figs. 4.14 and 4.15 show the shape of a fully clamped joint, so that the slope at the joint remains zero. Figs. 4.16 thru 4.18 are for a clamping pressure of 8.0E06 N/m^2.

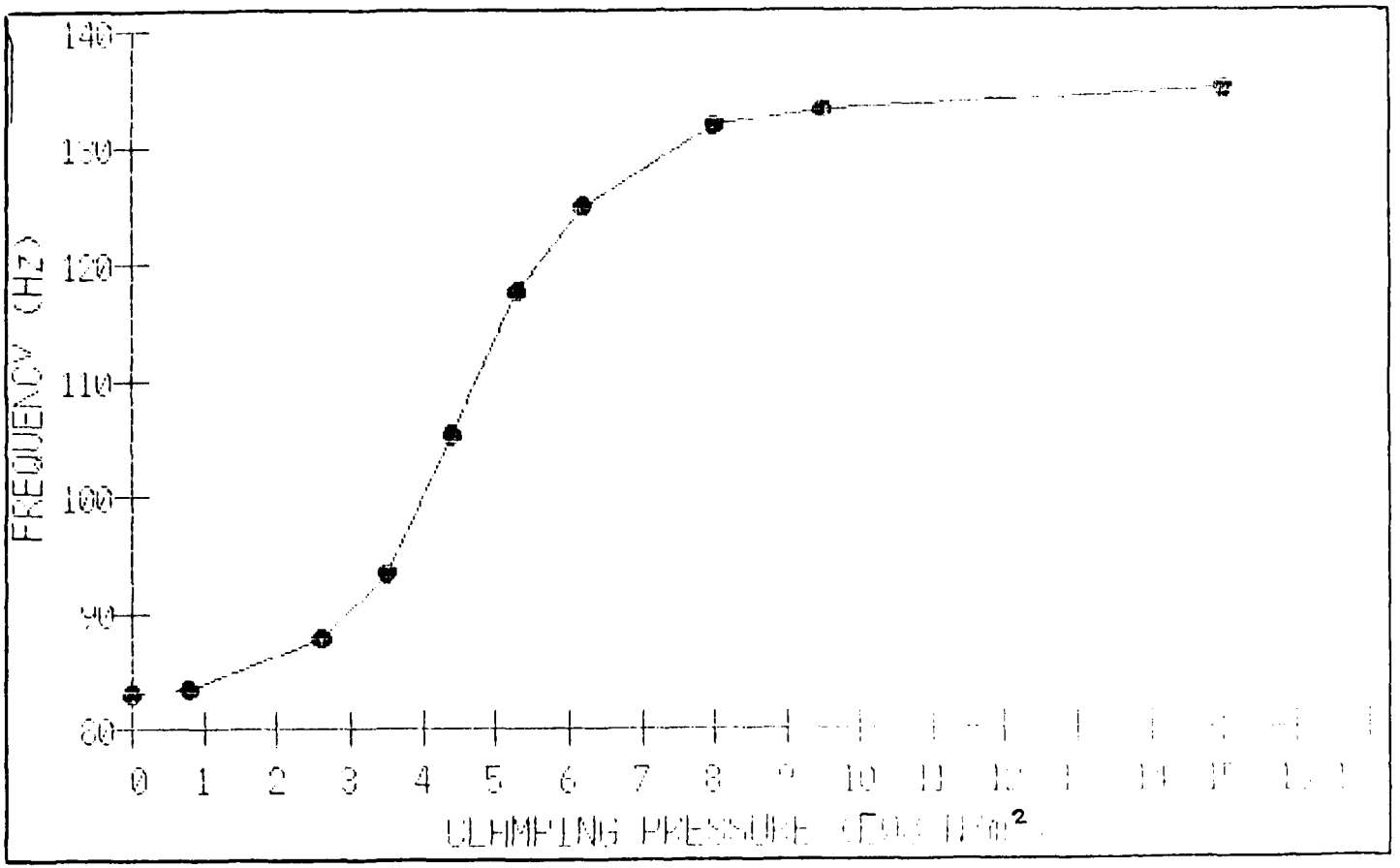

FIGURE 4.10 Frequency vs. Clamping Pressure

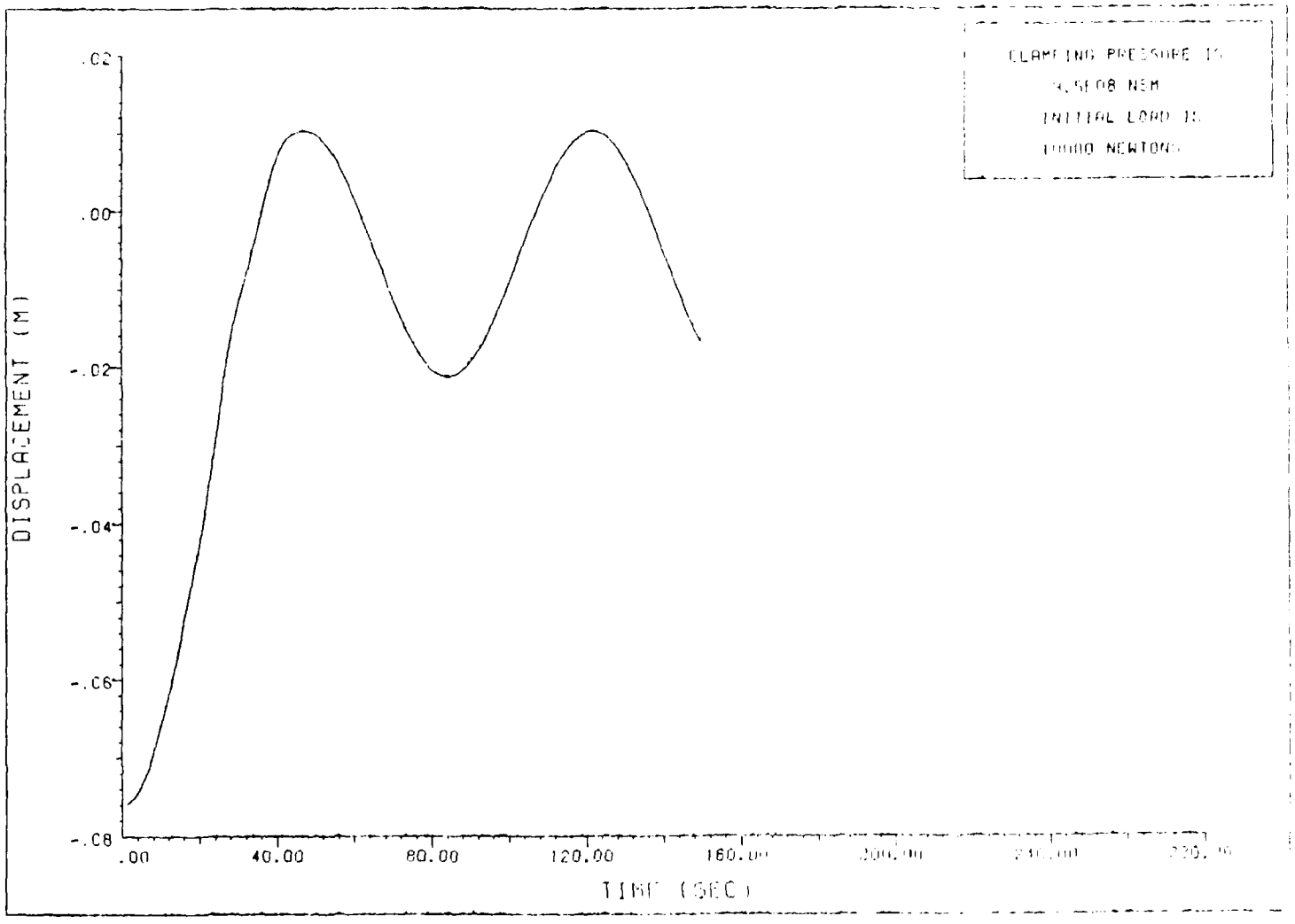

FIGURE 4.11 w_2 vs. Time

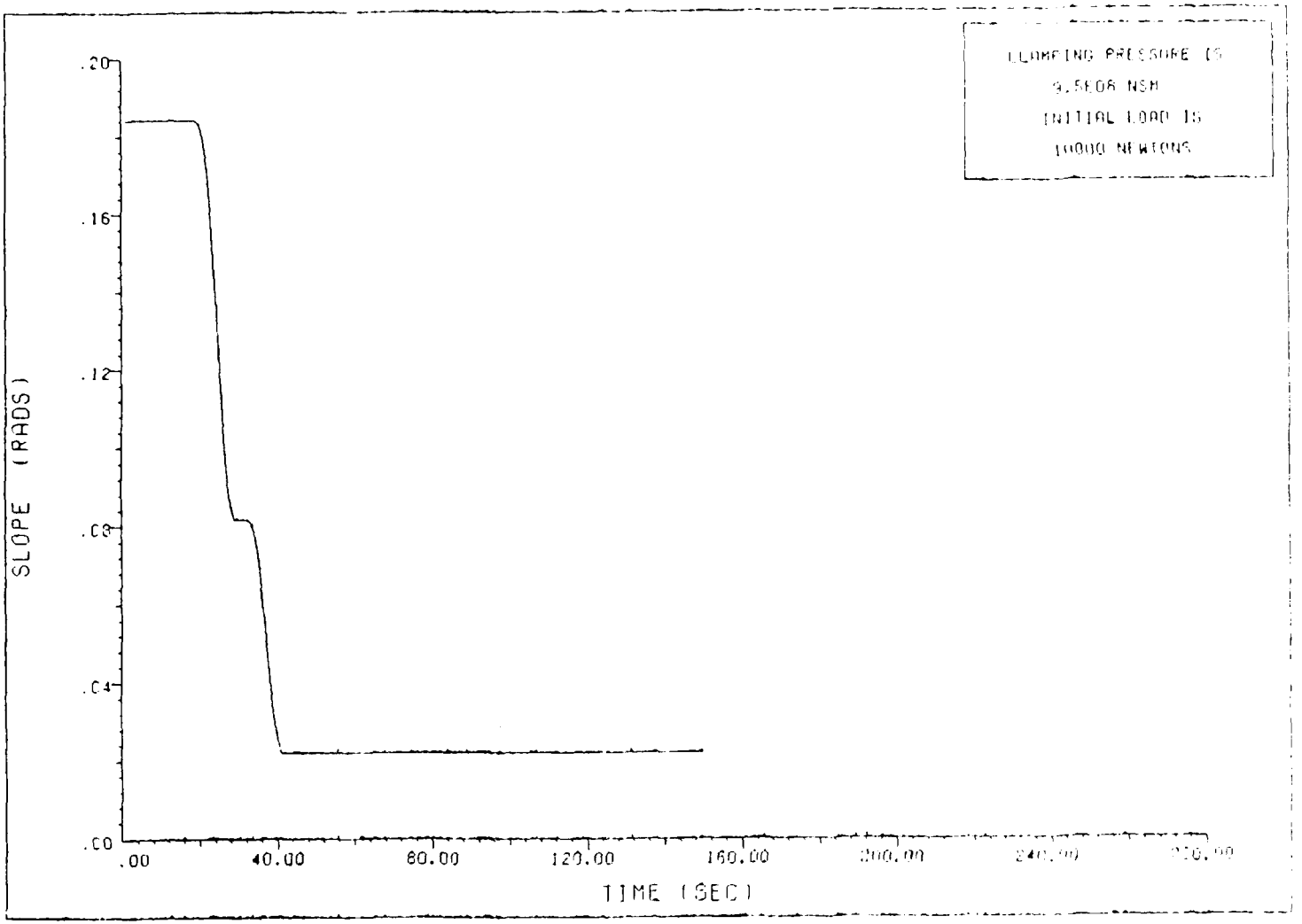

FIGURE 4.12 Slope vs. Time

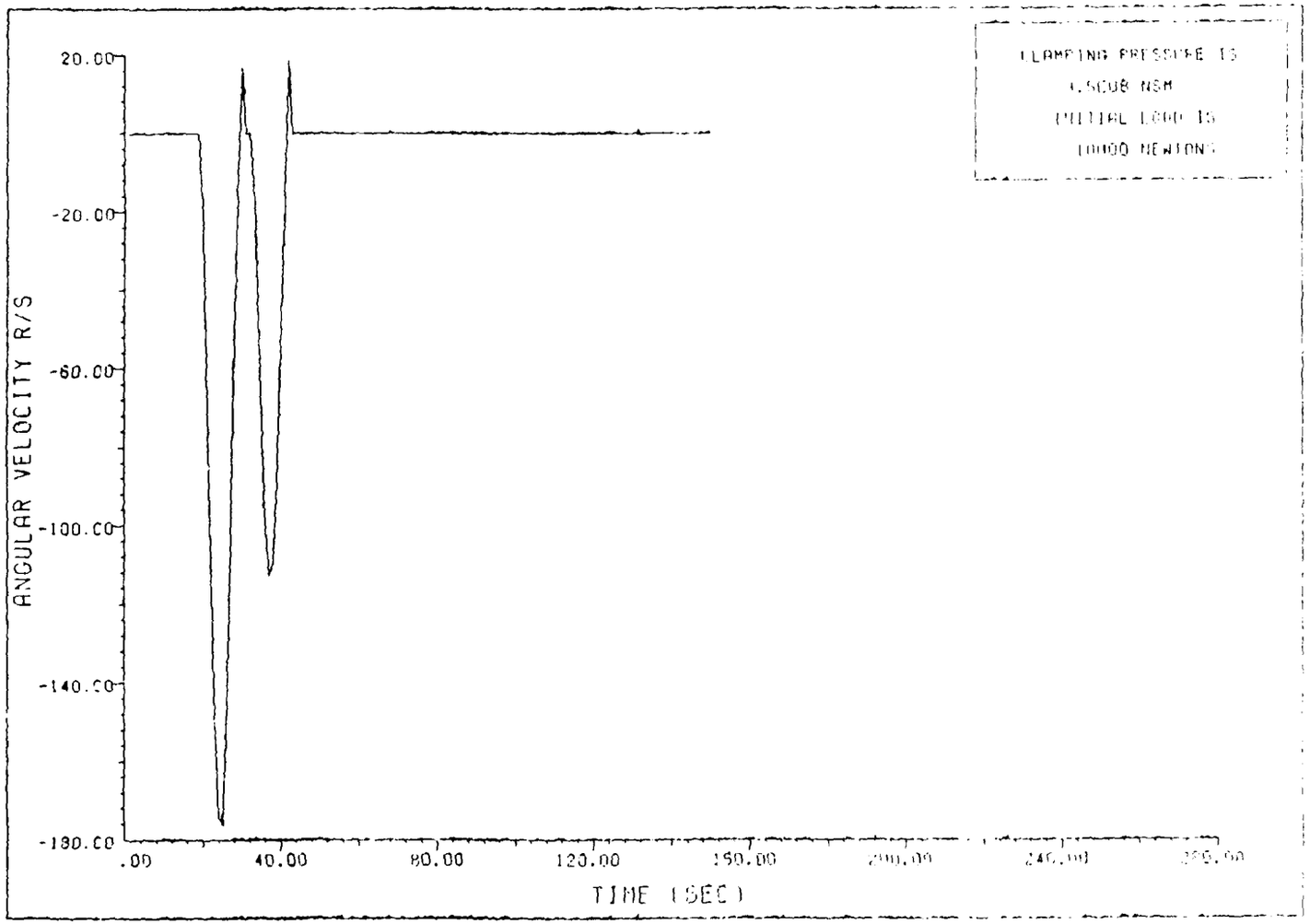

FIGURE 4.13 Angular Velocity vs. Time

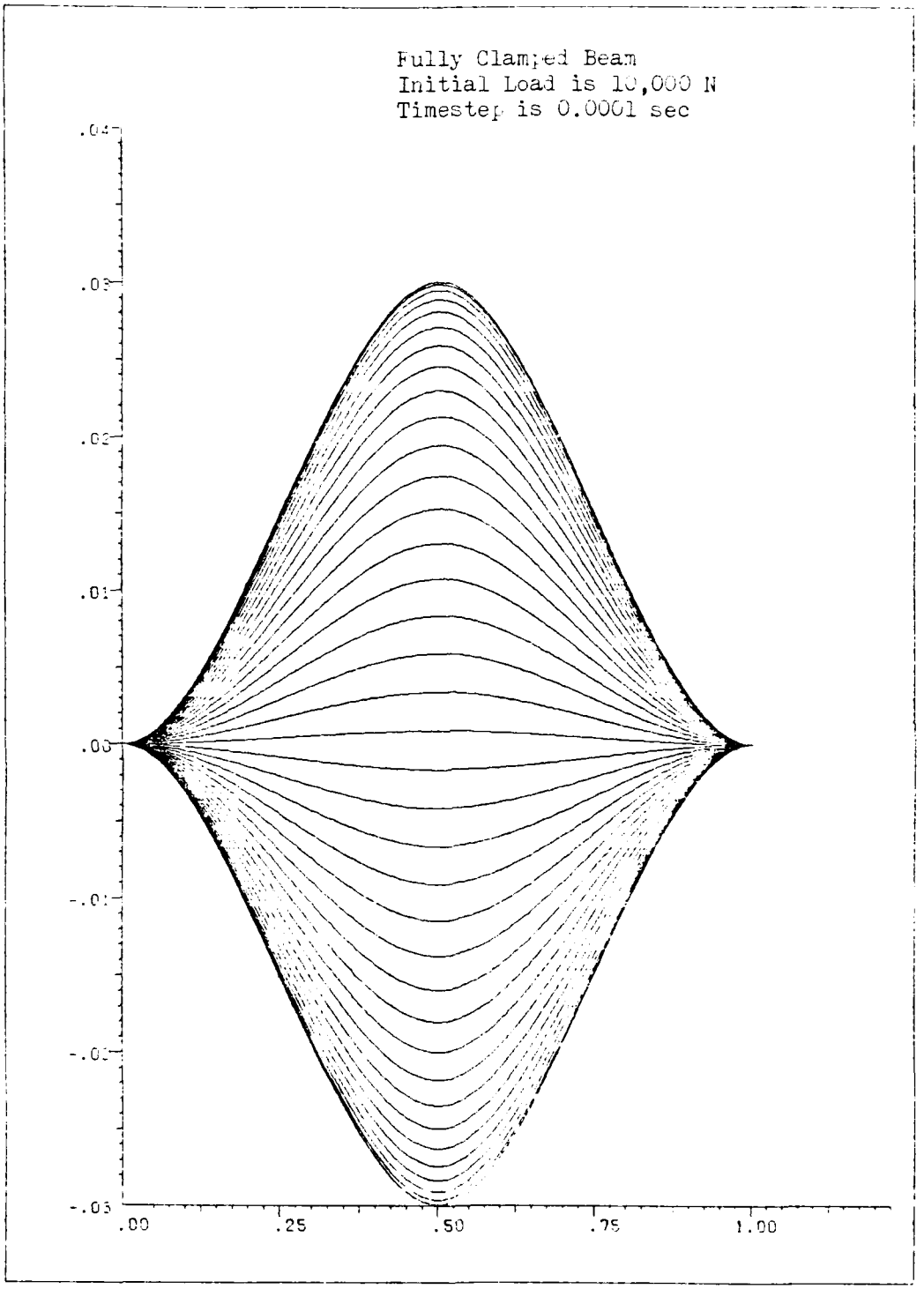

FIGURE 4.14 Beam Shape vs. Time
First Half-Cycle

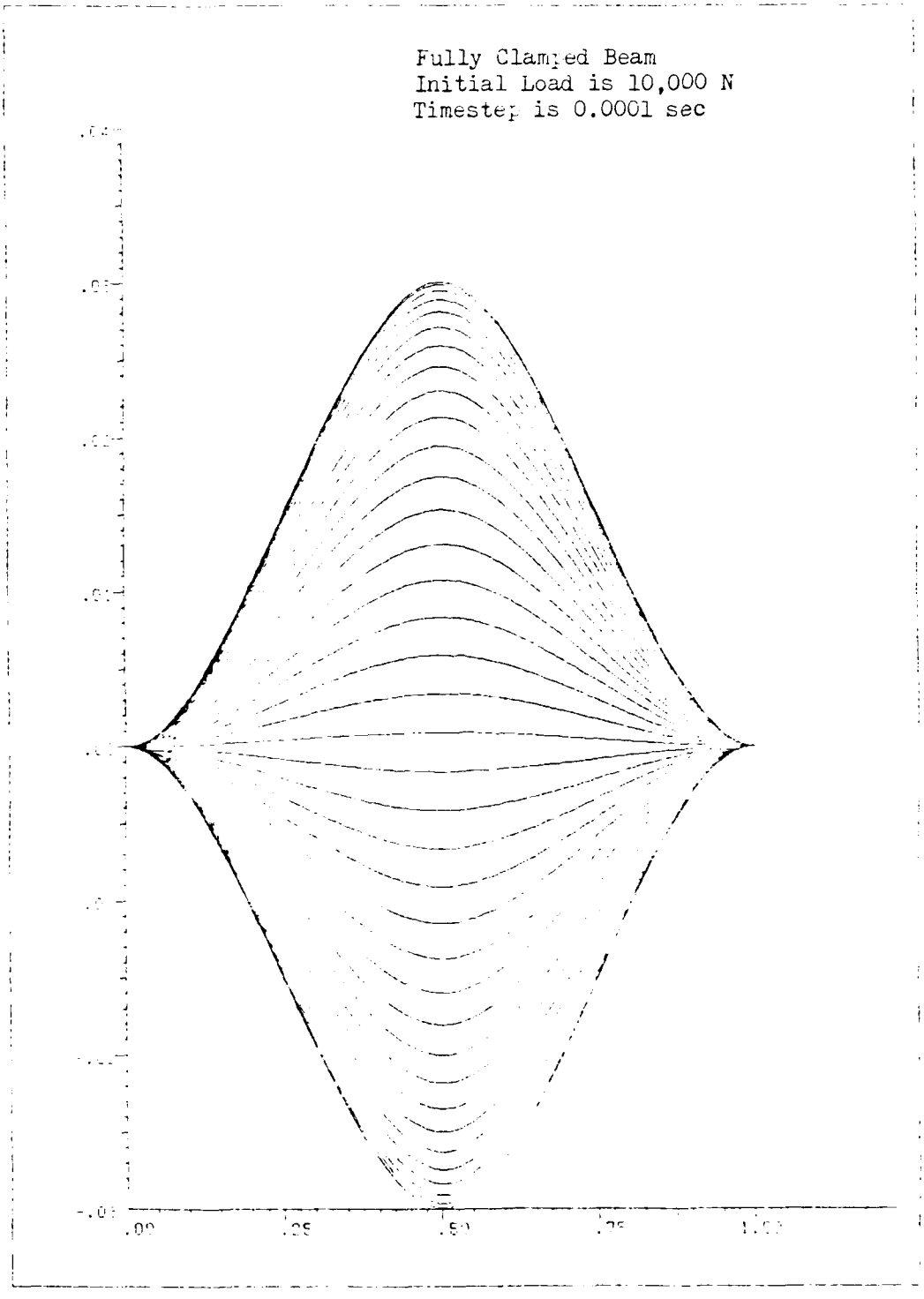

FIGURE 4.15 Beam Shape vs. Time
Second Half-Cycle

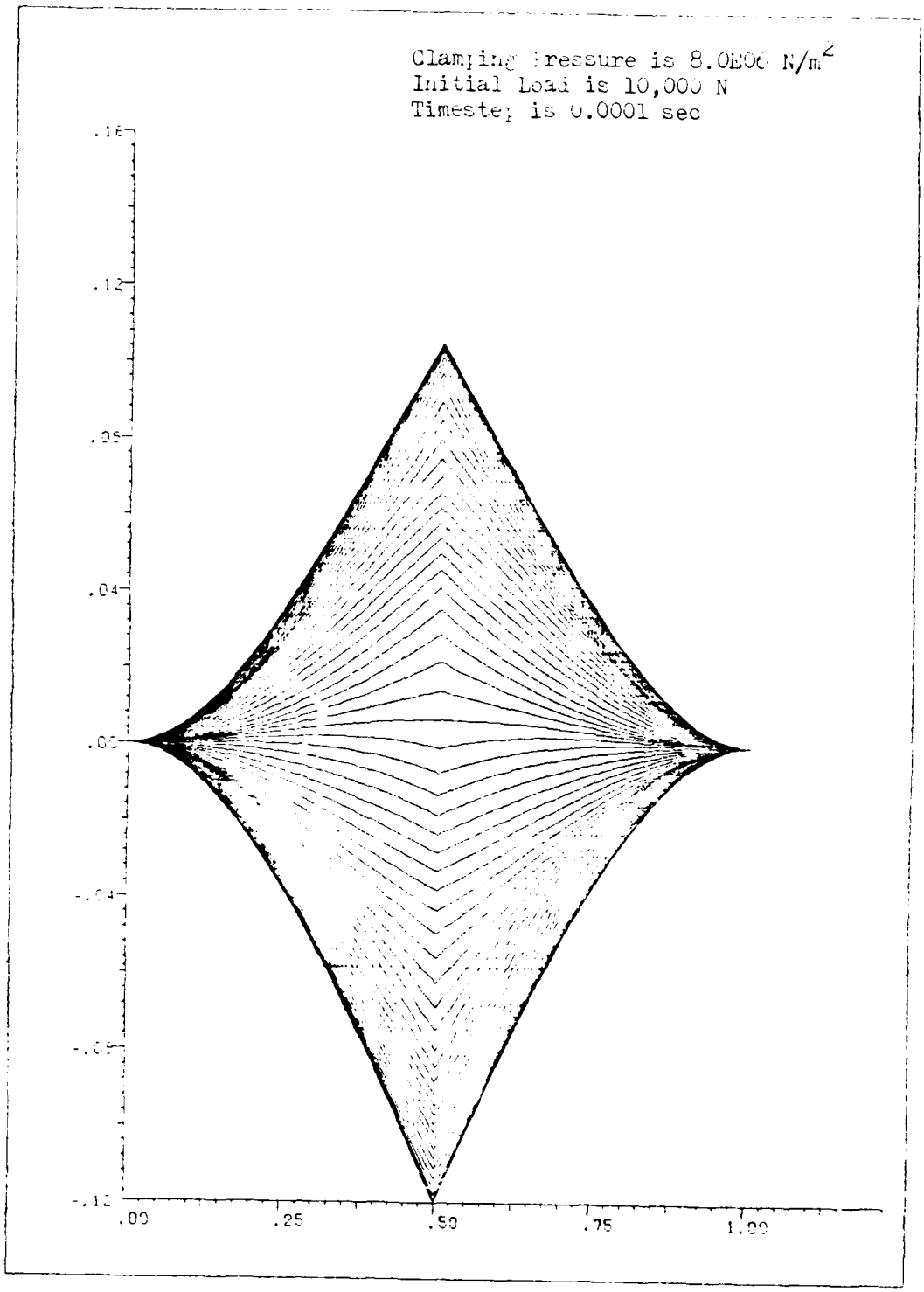

FIGURE 4.16 Beam Shape vs. Time
First Half-Cycle

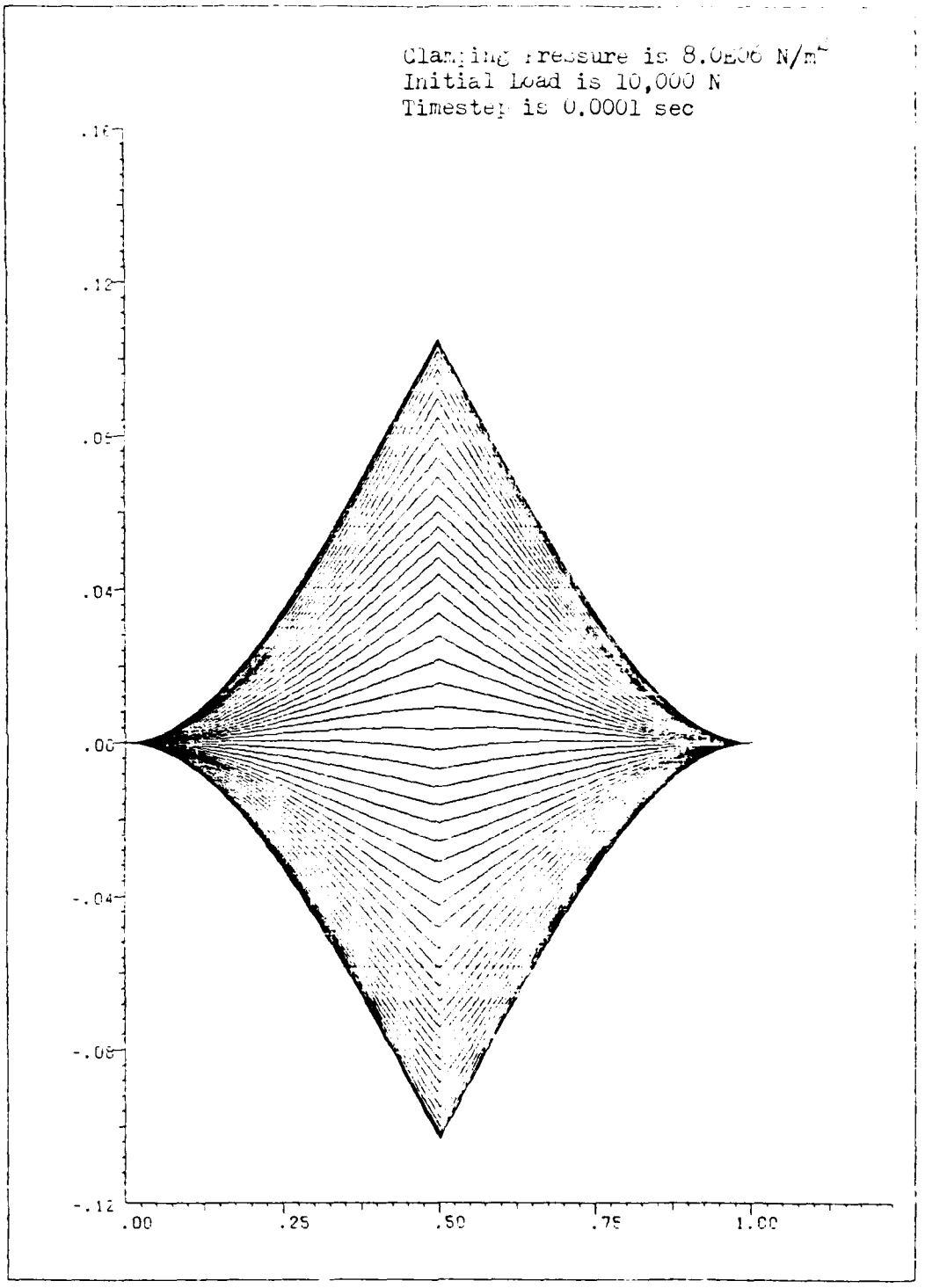

FIGURE 4.17 Beam Shape vs. Time
Second Half-Cycle

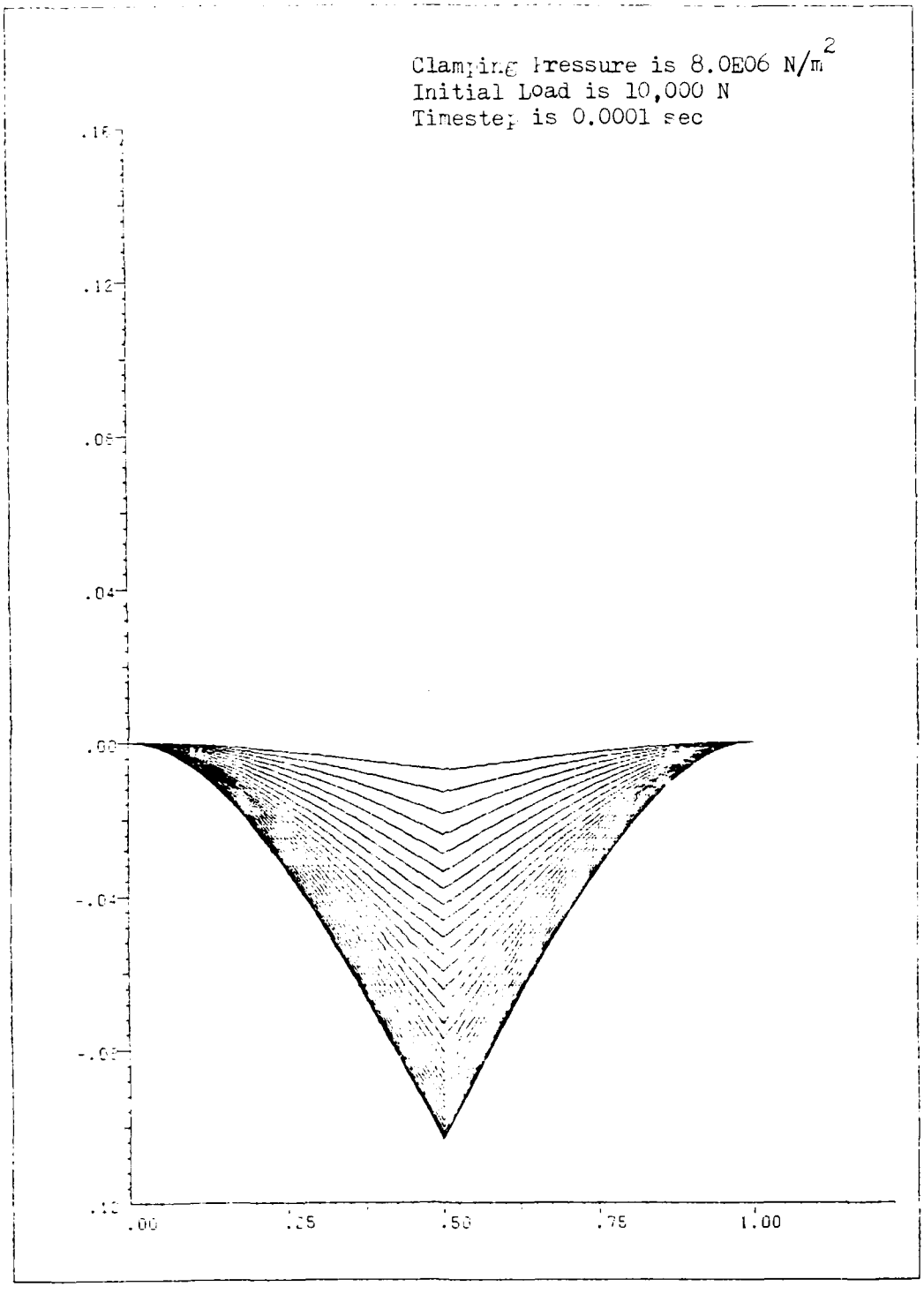

FIGURE 4.18 Beam Shape vs. Time
Third Half-Cycle

The slope and displacement are seen to vary significantly because the small value of M_{GROSS} is reached almost immediately. Figs. 4.19 and 4.20 are for a clamping pressure of 8.0E08 N/m^2. The displacement is damped a large amount in the first half-cycle, and the remainder is damped in the next half-cycle. The beam then vibrates with a fixed slope of -0.01018 rads at the joint.

Fig. 4.21 is a plot of moment versus slope for a moderately large clamping pressure of 8.0E08 N/m^2 and shows a hysteresis loop for the damping taking place at the joint. If the joint were excited by a cyclic load, the loop would be closed. Damping takes place on the horizontal lines of the loop, where the moment is constant and the slope is changing. This allows the energy loss to be calculated by multiplying the moment by the change in slope. Remember that before damping begins, the dynamic moment must equal the gross moment. The program was unable to reach the gross moment exactly, so some overshoot of the gross moment is seen. These are the spikes just before the line turns horizontal. One other spike is seen on the upper horizontal line. This is a point where the angular velocity changed sign and so the routine fixed the slope at the current value. However, at the next time step the moment exceeded the value of M_{GROSS}, so the slope was freed and damping continued. The loop starts at the far right and ends on the inner vertical line. The value of M_{GROSS} is not reached after the first two damping cycles for the initial

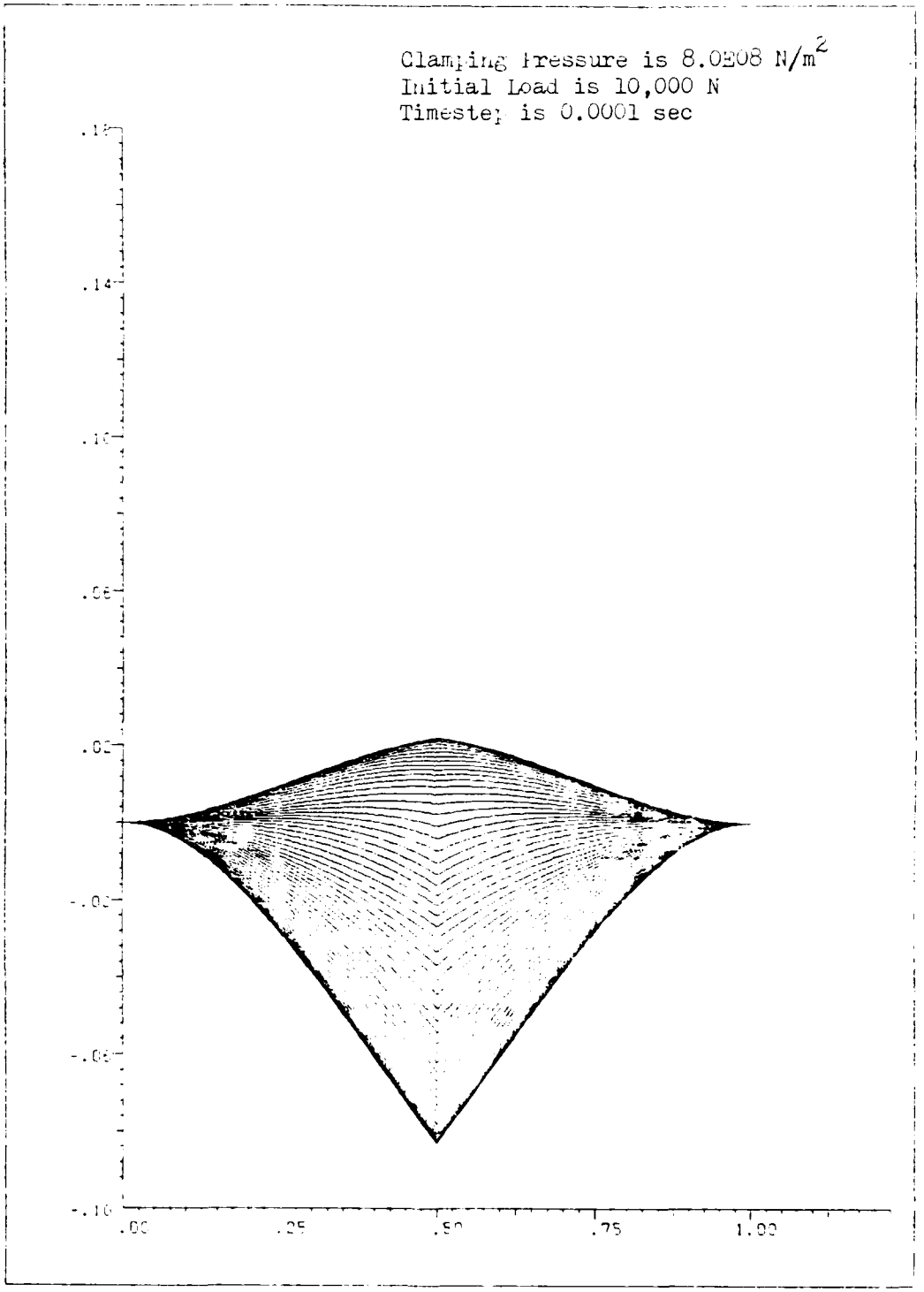

FIGURE 4.19 Beam Shape vs. Time
First Half-Cycle

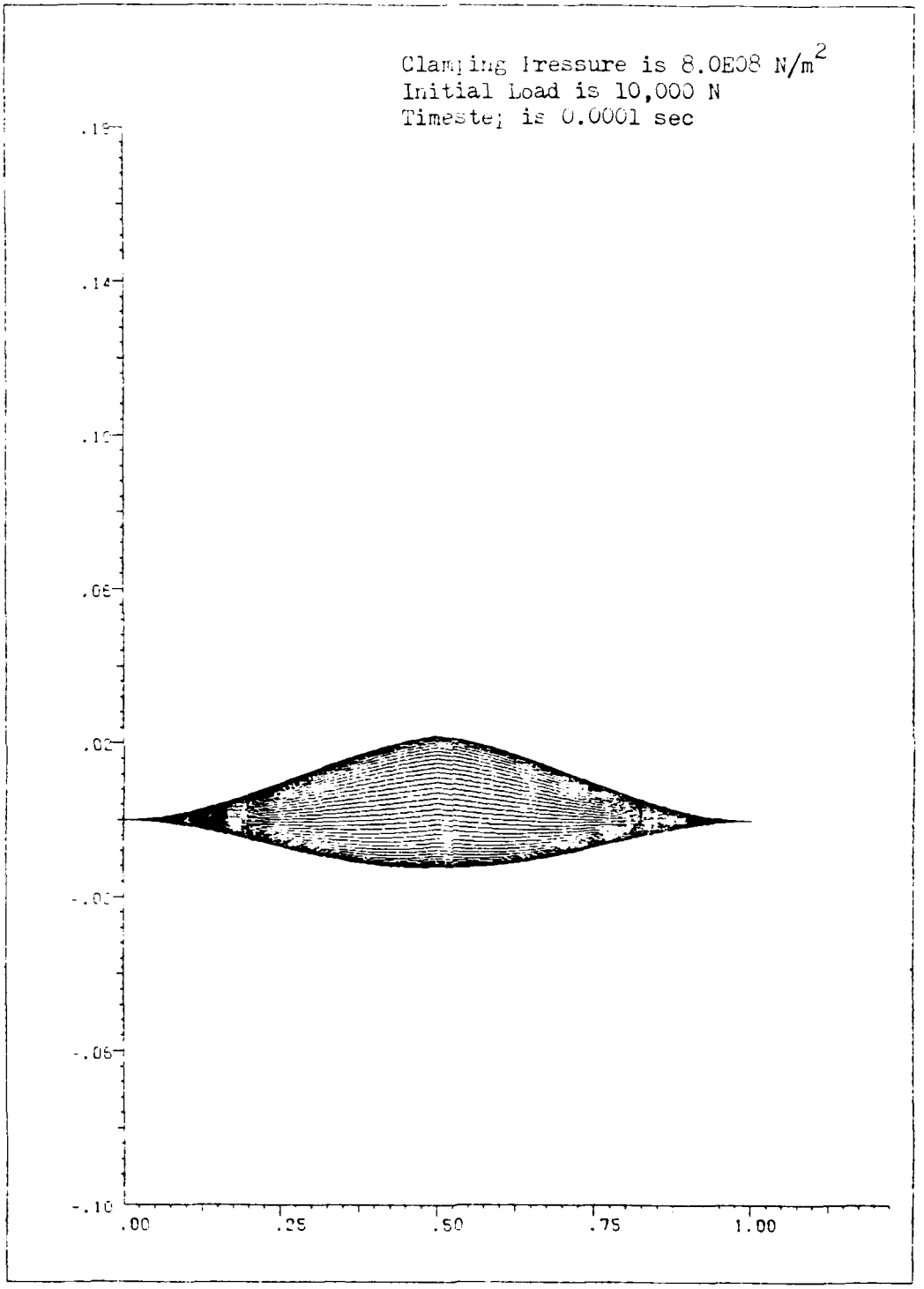

FIGURE 4.20 Beam Shape vs. Time
Second Half-Cycle

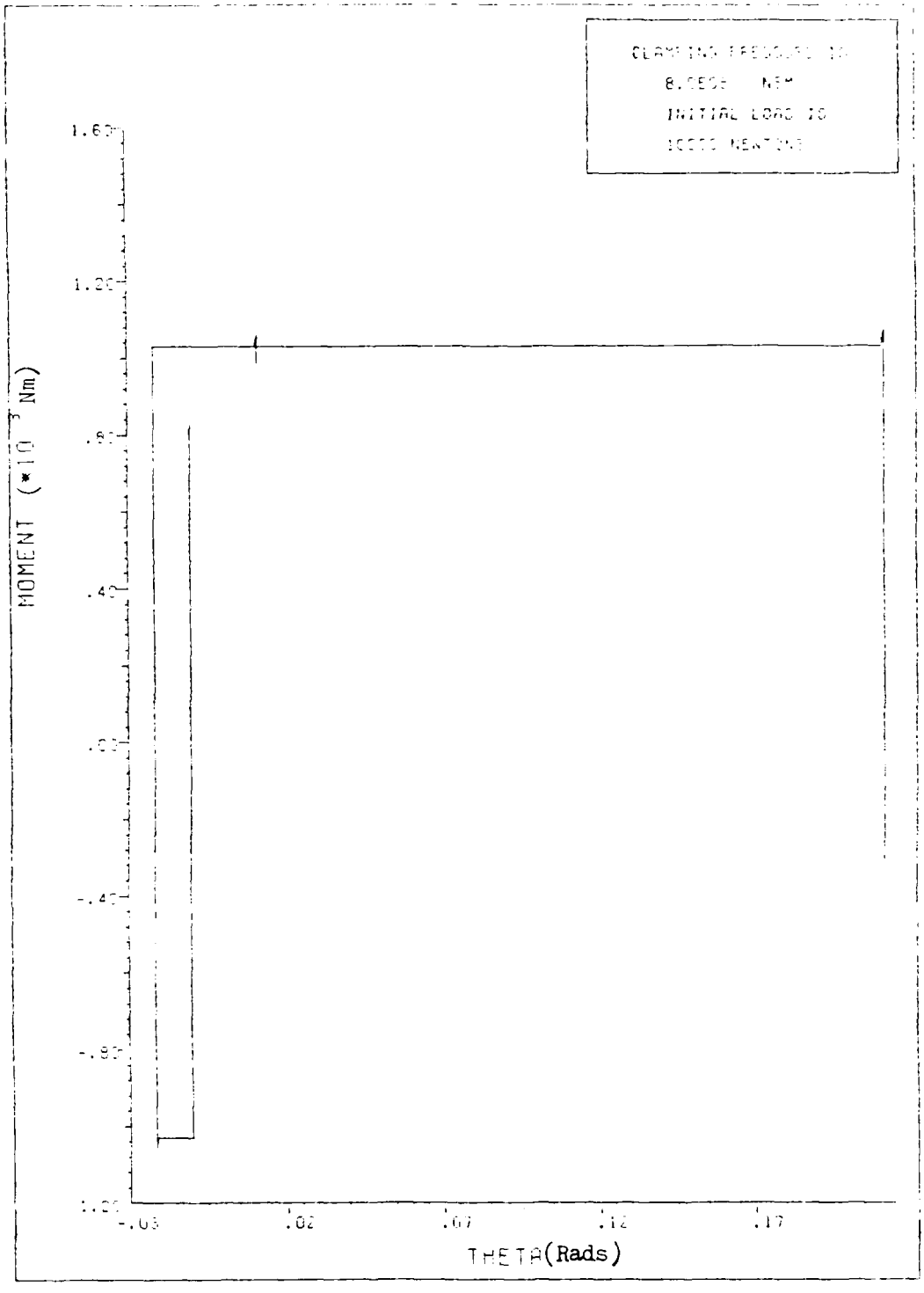

FIGURE 4.21 Hysteresis Loop

conditions given, so the moment varies up and down the line which indicates a constant slope of -0.01018 rads.

Table 4.1 shows the percent of energy lost during the first half-cycle and a full cycle for various clamping pressures and an initial applied load of 10,000 N. Note that the results for the first half-cycle show an increase in damping as clamping pressure increases. But, the numbers reach a maximum and then decrease for the damping done in one cycleas clamping pressure increases. This is better illustrated in the plot of Fig. 4.22.

CLAMPING PRESSURE	3.5 E08 $\frac{N}{m^2}$	4.4 E08 $\frac{N}{m^2}$	5.3 E08 $\frac{N}{m^2}$	6.2 E08 $\frac{N}{m^2}$	8.0 E08 $\frac{N}{m^2}$
INITIAL DEFLECTION	-0.10389 m	-0.099718m	-0.095543m	-0.091369 m	-0.08302 m
INITIAL SLOPE (RADS)	0.29544	0.27874	0.26205	0.24535	0.21195
INITIAL STRAIN ENERGY	452.945 Nm	419.783 Nm	388.340 Nm	358.454 Nm	305.983 Nm
ENERGY DISSIPATED 1ST HALF-CYCLE	212.290 Nm	243.252 Nm	258.049 Nm	253.920 Nm	240.589 Nm
ENERGY DISSIPATED 2ND HALF-CYCLE	126.720 Nm	119.573 Nm	85.137 Nm	65.856 Nm	11.876 Nm
%ENERGY DISSIPATED 1ST HALF-CYCLE	46.87	57.95	66.45	70.74	78.63
%ENERGY DISSIPATED ONE CYCLE	74.85	86.43	88.37	89.09	82.51

TABLE 4.1 Percent Energy Loss vs. Clamping Pressure

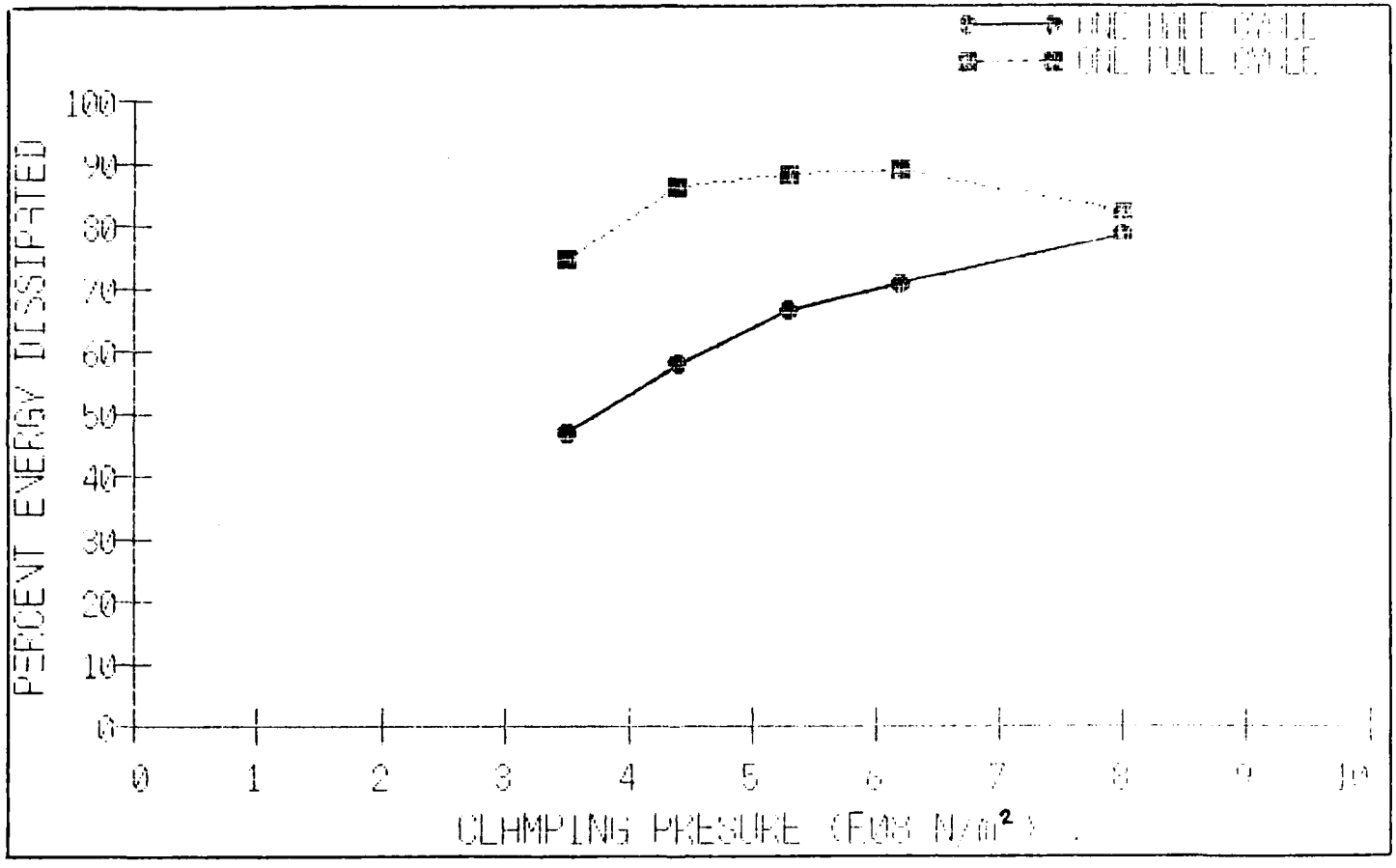

FIGURE 4.22 Percent Energy Loss vs. Clamping Pressure

CHAPTER 5

CONCLUSIONS

The finite element method is capable of predicting the amount of energy lost due to friction damping at the joint of a simple beam structure. It was able to calculate slopes, displacements, velocities, and accelerations, as well as the frequencies associated with them. Enough information was obtained that the actual shape of the beam could be plotted. The modified one-dimensional program provided data that appeared accurate despite the inadequacy of the original program to handle the independent rotation degrees of freedom at the joint. The problem was simplified by the assumptions made, but the results have opened the door for continued investigation of the friction damping phenomenon.

A higher mode of vibration was seen on the angular velocity versus time plot, but the accuracy for the frequency is debatable because only one element was used. The use of only one element made the beam stiffer than it really was, therefore the frequency of the second mode would be higher than it should be. This could be corrected by using two elements. Higher modes would be introduced, and their accuracy would depend on the number of elements used.

The errors encountered by not using smaller time steps and actually stepping over the values of M_{GROSS} and the angular velocity when turning the damping mechanism on and

off did not affect the results obtained. The hysteresis loop shows that the friction moment was exceeded rather than equaled, but at the next time step the value at the joint is the value of M_{GROSS}. So the time step chosen was more than adequate to give accurate results.

The displacement, w_2, is seen to decrease as the clamping pressure increases. This correlates to the percent energy loss for a half-cycle and a full cycle. The percent energy loss for the first half-cycle increases as the clamping pressure increases. However, it reaches a maximum and begins to decrease as clamping pressure increases for a full cycle.

The frequency increases as the clamping pressure increases. This can be explained by the beam becoming stiffer and the period decreasing. In other words, the beam vibrates faster. For a given clamping pressure, the frequency remains constant for any initial applied load. The amplitude varies with the load, but the frequency does not.

The accuracy of the results are unknown as no data was available to compare with. However, the trends observed indicated that the data obtained was a good first estimate for the amount of friction damping.

CHAPTER 6

RECOMMENDATIONS

This thesis has opened the door for many follow-on studies to be accomplished. As many questions as were answered, many more new ones were asked. Some additional work that could be completed in this area is:

1. A two-dimensional finite element program could be used to verify the results obtained by the modified one-dimensional program.

2. An investigation into the higher modes could be made using more elements in the beam model.

3. The assumptions could be relaxed to allow more variables to come into play, such as;

a. Allow the clamping pressure to vary from a maximum at the point of application to some lesser away from the point of application.

b. Allow partial slip. This would mean the joint would always be in some form of slip once a break-away value was exceeded.

c. Allow the coefficient of friction to vary with time

to simulate wearing of the contact surfaces.

4. Finally, the problem should be accomplished experimentally to obtain some laboratory values to compare against the numerical integration methods.

APPENDIX A

Beam is made of steel

$\mu = 0.3$ $\rho = 7827.1093\ Kg/m^3$ $E = 2.0E11\ N/m^2$

Area of cross-section = bh = (0.012/m)(0.0254m)

$= 3.2258E-04\ m^2$

$\rho A = 2.5248689\ Kg/m$

$I = (1/12)bh^3 = (1/12)(0.012/m)(0.0254m)^3 = 1.7342976E-08\ m^4$

$EI = 3468.5952\ Nm^2$

Area of contact surface = $\pi R^2 = \pi(.012/m)^2 = 5.0670746E-04\ m^2$

$M_{GROSS} = 2\pi\mu PR^3/3 = (1.2870376E-06\ m^3)(P\ N/m^2)\ Nm$

APPENDIX B

The differential equation for the dynamic problem consists of the following terms:

$$\begin{bmatrix} M_{11} & M_{12} & M_{13} & M_{14} \\ M_{21} & M_{22} & M_{23} & M_{24} \\ M_{31} & M_{32} & M_{33} & M_{34} \\ M_{41} & M_{42} & M_{43} & M_{44} \end{bmatrix} \begin{Bmatrix} \ddot{w}_1 \\ \ddot{\theta}_1 \\ \ddot{w}_2 \\ \ddot{\theta}_2 \end{Bmatrix} + \begin{bmatrix} K_{11} & K_{12} & K_{13} & K_{14} \\ K_{21} & K_{22} & K_{23} & K_{24} \\ K_{31} & K_{32} & K_{33} & K_{34} \\ K_{41} & K_{42} & K_{43} & K_{44} \end{bmatrix} \begin{Bmatrix} w_1 \\ \theta_1 \\ w_2 \\ \theta_2 \end{Bmatrix} = \begin{Bmatrix} F_1 \\ M_1 \\ F_2 \\ M_2 \end{Bmatrix}$$

The clamped boundary conditions at the first node ($w_1 = \theta_1 = 0$) allow the following simplification to be made:

$$\begin{bmatrix} M_{33} & M_{34} \\ M_{43} & M_{44} \end{bmatrix} \begin{Bmatrix} \ddot{w}_2 \\ \ddot{\theta}_2 \end{Bmatrix} + \begin{bmatrix} K_{33} & K_{34} \\ K_{43} & K_{44} \end{bmatrix} \begin{Bmatrix} w_2 \\ \theta_2 \end{Bmatrix} = \begin{Bmatrix} F_2 \\ M_2 \end{Bmatrix}$$

Therefore, the moment required to compare against M_{GROSS} is

$$M_2 = M_{43}\ddot{w}_2 + M_{44}\ddot{\theta}_2 + K_{43}w_2 + K_{44}\theta_2$$

The displacement and acceleration vectors are obtained by numerical analysis, the Newmark Beta method in this case.

APPENDIX C

```
      SUBROUTINE STRESS(NPE,NDF,IBEAM,IELEM,W0,ELX,N,NEM,IFLAG,NT,
     *VBF,INITIAL,BX0,KICK,FORCE,R,FRICTION,ITEM,IBF,VBDY,IBDY,
     *KOUNT,GF,GF1,GF2,T)
C
C     ---------------------------------------------------------
C       X.........GLOBAL COORDINATE
C       XI........LOCAL COORDINATE
C       SF........ELEMENT INTERPOLATION FUNCTIONS
C       GDSF......FIRST DERIVATIVE OF SF W.R.T. GLOBAL COORDINATE
C       GDDSF....SECOND DERIVATIVE OF SF W.R.T. GLOBAL COORDINATE
C        W0........COLUMN OF GENERALIZED DISPLACEMENTS
C        W.........INTERPOLATED GENERALIZED DISPLACEMENT
C        DW........FIRST DERIVATIVE OF W: DW/DX
C        DDW.......SECOND DERIVATIVE OF W: D(DW)/DX
C
C       NOTE: W,  DW, AND DDW ARE COMPUTED AT NINE POINTS OF EACH
C             ELEMENT (DW AND DDW ARE NOT EXPECTED TO BE ACCURATE
C             AT THE NODAL POINTS OF THE ELEMENT)
C     ---------------------------------------------------------
C
       IMPLICIT REAL*8(A-H,O-Z)
       COMMON/STRS/XG(18),W(18),DW(18),DDW(18),NBDY,NBF,B43,B44,
     *G43,G44,VT,VT1
       COMMON/SHP/SF(4),GDSF(4),GDDSF(4),GJ
       DIMENSION   GAUSS(9),W0(4),ELX(4),VBF(11),IBF(11),VBDY(11),
     *IBDY(11),GF(4),GF1(4),GF2(4)
       DATA GAUSS/-1.0D0,-0.75D0,-0.50D0,
     *-0.25D0,0.0D0,0.25D0,0.50D0,
     *           0.75D0,1.0D0/
C
       NET=NPE
       IF(IELEM .EQ. 0)NET=4
       H = ELX(NPE)-ELX(1)
       DO 85 NI=1,9
       XI = GAUSS(NI)
       CALL SHAPE(XI,H,NPE,NET,IELEM)
       NN=(N-1)*9+NI
       XG(NN) = 0.5*H*(1.0+XI)+ELX(1)
       W(NN)=0.0
       DW(NN)=0.0
       DDW(NN)=0.0
       DO 60 I=1,NET
       W(NN) = W(NN) + SF(I)*W0(I)
       DW(NN)=DW(NN)+GDSF(I)*W0(I)
       IF(IELEM .NE. 0)GOTO 60
       DDW(NN)=DDW(NN)+GDDSF(I)*W0(I)
   60  CONTINUE
       IF(IBEAM.EQ.0)GOTO 85
       IF(N.NE.1.OR.NI.NE.9)GOTO 85
```

```
      IF(ITEM.GE.1)GOTO 55
      ZGROSS=(2*FRICTION*3.14159*FORCE*R**3)/3
C     PRINT*,'ZGROSS= ',ZGROSS
      Z=BX0*DDW(9)
C     PRINT*,'      Z= ',Z
      IF(Z.LE.ZGROSS)GOTO 85
      NBDY=2
      NBF=2
      IBF(2)=4
      VBF(2)=-ZGROSS
      IFLAG=1
      GOTO 84
   55 ZGROSS=(2*FRICTION*3.14159*FORCE*R**3)/3
      PRINT*,' ZGROSS= ',ZGROSS
      Z=G43*GF2(3)+G44*GF2(4)+B43*GF(3)+B44*GF(4)
      PRINT*,'       Z= ',Z
      IF(VT1.GT.0.0)THEN
      IF(VBF(1).GT.0.0)GOTO 75
      IF(ABS(Z).LE.ZGROSS)GOTO 84
      GOTO 50
   75 NBDY=3
      NBF=0
      IBDY(3)=4
      VBDY(3)=W0(4)
      GF1(4)=0.0
      GF2(4)=0.0
      VBF(1)=0.0
      GOTO 84
   50 NBDY=2
      NBF=1
      IBF(1)=4
      VBF(1)=-ZGROSS
      GOTO 84
      ENDIF
      IF(VBF(1).LT.0.0)GOTO 75
      IF(ABS(Z).LE.ZGROSS)GOTO 84
      IF(Z.LT.0.0)GOTO 50
      NBDY=2
      NBF=1
      IBF(1)=4
      VBF(1)=ZGROSS
   84 PRINT*,'VBF(1)= ',VBF(1)
   85 CONTINUE
      PRINT*,'GO ON TO NEXT TIME STEP; NT,KOUNT = ',NT,KOUNT
   90 RETURN
      END
```

BIBLIOGRAPHY

1. Beards, C.F., "Damping In Structural Joints," Shock and Vibration Digest, Vol 11(9): 35-41, 1979.

2. Beards, C.F., "Damping In Structural Joints," Shock and Vibration Digest, Vol 14(6): 9-10, 1982.

3. Beards, C.F., "Some effects of Interface Preparation on Frictional Damping in Joints," International Journal of Machine Tool Design and Research, Vol 15: 77-83, 1975.

4. Beards, C.F., Williams, J.L., "The Damping of Structural Vibration by Rotational Slip in Joints," Journal of Sound and Vibration, Vol 53(3): 333-340, 1977.

5. Beards, C.F., "The Damping of Structural Vibration by Controlled Interfacial Slip in Joints," Journal of Vibration, Acoustics, Stress, and Reliability in Design, Vol 105: 369-373, 1983.

6. Beards, C.F., "The Control of Frame Vibration by Friction Damping in Joints," Journal of Vibration, Acoustics, Stress, and Reliability in Design, Vol 107: 26-32, 1985.

7. Cernica, J.N., Strength of Materials, New York, Holt, Rinehart and Winston, Inc., 1966.

8. Cook, R.D., Concepts and Applications of Finite Element Analysis, New York, John Wiley and Sons, 1981.

9. Dym, Clive L., Shames, Irving H., Solid Mechanics A Variational Approach, New York, Mcgraw Hill, 1973.

10. Greenwood, D.T., Principles of Dynamics, New Jersey, Prentice-Hall, Inc., 1965.

11. Lazan, B.J., "Review of Structural Damping Mechanisms," Wright Air Development Center Technical Report 59-676, 1961.

12. Meirovitch, L., Elements of Vibration Analysis, USA, McGraw-Hill, Inc., 1975.

13. Nishiwaki, N., Masuko, M., Ito, Y., Okumura, I, "A Study on Damping Capacity of a Jointed Cantilever Beam," Journal of the Society for Mechanical Engineers, Vol 21: 524-531, 1978.

14. Plunkett, R., "Friction Damping," Damping Applications in Vibration Control, Ed. P.J. Torvik, AMD Vol 38, American Society of Mechanical Engineers, 1980.

15. Reddy, J.N., An Introduction to the Finite Element Method, New York, McGraw-Hill Inc., 1984.

16. Richardson, R.S.H., Nolle, H., "Energy Dissipation in Rotary Structural Joints," Journal of Sound and Vibration, Vol 54(4): 577-588, 1977.

17. Shigley, J.E., Mechanical Engineering Design, New York, McGraw-Hill, Inc., 1972.

18. Snowden, J.C., Vibration and Shock in Damped Mechanical Systems, New York, John Wiley and Sons, Inc., 1968.

19. Srinivasan, A.V., Cassenti, B.N., Cutts, D.G., "Characteristics of Dry Friction Damping," United Technologies Research Center, Connecticut.

20. Timoshenko, S., Young, D.H., Weaver, W., Jr., Vibration Problems in Engineering, New York, John Wiley and Sons, 1974.

21. Torvik, P.J., "Damping: Its Application in Transportation Vehicles," Materials on the Move, Vol 6, 1974.

22. Wilson, E. L., Bathe, Klaus-Jurgen, Numerical Methods in Finite Element Analysis, Englewood Cliffs, New Jersey, Prentice Hall, 1976.

Robert P. Donnelly, Jr. was born in Harlingen, Texas on 11 September 1955. He graduated as one of three outstanding graduates from Torrejon American High School in Madrid, Spain in 1973. On 1 June 1977 he received a B.S. in Engineering Mechanics from the United States Air Force Academy. After attending helicopter flight training at Ft. Rucker, Alabama he was assigned to the 20th Special Operations Squadron at Hurlburt Field, Florida. In 1981, he was stationed at Plattsburgh AFB, New York with Detachment 18, 40th Aerospace Rescue and Recovery Squadron where he held the jobs of Flight Examiner and Operations Officer. In May 1984 he came to the Air Force Institute of Technology to pursue a M.S. Degree in Aeronautical Engineering.

He married Miss Diana E. Bailey of Ft. Rucker in 1980. They have two children; Rebecca Jeanne and Rachael Marie.

Permanent mailing address:

c/o Robert Donnelly
1624 Waltz Way
Midwest City, OK
73130

UNCLASSIFIED

SECURITY CLASSIFICATION OF THIS PAGE

AD-A163975

REPORT DOCUMENTATION PAGE

1a REPORT SECURITY CLASSIFICATION: UNCLASSIFIED	1b RESTRICTIVE MARKINGS
2a SECURITY CLASSIFICATION AUTHORITY	3 DISTRIBUTION/AVAILABILITY OF REPORT: Approved for public release; distribution unlimited
2b DECLASSIFICATION/DOWNGRADING SCHEDULE	
4 PERFORMING ORGANIZATION REPORT NUMBER(S): AFIT/GAE/AA/85D-5	5 MONITORING ORGANIZATION REPORT NUMBER(S)
6a NAME OF PERFORMING ORGANIZATION: School of Engineering; 6b OFFICE SYMBOL (If applicable): AFIT/EN	7a NAME OF MONITORING ORGANIZATION
6c ADDRESS (City, State and ZIP Code): Air Force Institute of Technology, Wright Patterson AFB, Ohio 45433	7b ADDRESS (City, State and ZIP Code)
8a NAME OF FUNDING/SPONSORING ORGANIZATION; 8b OFFICE SYMBOL (If applicable)	9 PROCUREMENT INSTRUMENT IDENTIFICATION NUMBER
8c ADDRESS (City, State and ZIP Code)	10 SOURCE OF FUNDING NOS: PROGRAM ELEMENT NO; PROJECT NO; TASK NO; WORK UNIT NO
11 TITLE (Include Security Classification): See Box 19	
12 PERSONAL AUTHOR(S): Robert P. Donnelly, Jr., CAPT, USAF	
13a TYPE OF REPORT: MS Thesis; 13b TIME COVERED: FROM _____ TO _____; 14 DATE OF REPORT (Yr., Mo., Day): 1985 December; 15 PAGE COUNT: 69	
16 SUPPLEMENTARY NOTATION	

17 COSATI CODES			18 SUBJECT TERMS (Continue on reverse if necessary and identify by block number)
FIELD	GROUP	SUB GR	Damping, Joint Damping, Friction Damping, Coulomb Damping.
13	05		

19 ABSTRACT (Continue on reverse if necessary and identify by block number)

Title: The Effect of Energy Dissipation Due to Friction at the Joint of a Simple Beam Structure

Thesis Advisor: Ronald L. Hinrichsen, CAPT, USAF
Department of Aeronautics and Astronautics

Approved for public release: IAW AFR 190-1.
LYNN E. WOLAVER 16 JAN 86
Dean for Research and Professional Development
Air Force Institute of Technology (AFIT)
Wright-Patterson AFB OH 45433

20 DISTRIBUTION/AVAILABILITY OF ABSTRACT	21 ABSTRACT SECURITY CLASSIFICATION
UNCLASSIFIED/UNLIMITED ☒ SAME AS RPT ☐ DTIC USERS ☐	UNCLASSIFIED

22a NAME OF RESPONSIBLE INDIVIDUAL	22b TELEPHONE NUMBER (Include Area Code)	22c OFFICE SYMBOL
Ronald L. Hinrichsen, CAPT, USAF	513-255-3069	AFIT/ENY

DD FORM 1473, 83 APR EDITION OF 1 JAN 73 IS OBSOLETE

UNCLASSIFIED

SECURITY CLASSIFICATION OF THIS PAGE

The Strategic Defense Initiative has generated new interest in the development of more stable space structures. This interset has increased the need for more detailed knowledge of the behavior of engineering structures under dynamic loading. Interests lie in decreasing the amount of vibration by both passively and actively damping the structure. A means exists to passively damp structures by friction damping resulting from relative slip between joint interfaces. It may be feasible to increase the damping in a structure by allowing more friction damping than is normal and thereby controlling the vibration response.

This study incorporates friction damping in a one-dimensional model. Finite element techniques are used to accomplish the numerical analysis. A clamped-clamped beam is used as the physical model. The mid-point of the two element beam is allowed to slip in rotation, but not in translation. Because the one-dimensional program cannot handle rotations at continuous nodes, the beam is modeled by symmetry about the joint and a cantilever beam with an applied end moment is studied.

Results for the response of a beam in vibration are presented showing displacement of the joint, relative rotation at the joint, and relative angular velocity at the joint; all versus time. Various clamping pressures and initial loads are explored. Diagrams of the beam shape versus time show the shape the beam takes on when slip occurs at the joint. Frequency calculations show that the period of the response is affected by clamping pressure, but not by the initial loading. Energy loss calculations are presented for various clamping pressures.

END

FILMED

4-86

DTIC